Rapid widespread declines of an abundant coastal shark

Lindsay N.K. Davidson[1*], Philina A. English[1], Jacquelynne R. King[1], Paul Grant[2], Ian G. Taylor[4], Lewis A.K. Barnett[3], Vladlena Gertseva[4], Cindy A. Tribuzio[5], and Sean C. Anderson[1]

[1]Pacific Biological Station, Fisheries and Oceans Canada, Nanaimo, BC, Canada
[2]Institute of Ocean Sciences, Fisheries and Oceans Canada, Sidney, BC, Canada
[3]Resource Assessment and Conservation Engineering Division, NOAA Alaska Fisheries Science Center, Seattle, WA, USA
[4]Fishery Resource Analysis and Monitoring Division, Northwest Fisheries Science Center, National Marine Fisheries Service, Seattle, WA, USA
[5]Auke Bay Laboratories, Alaska Fisheries Science Center, National Marine Fisheries Service, NOAA, 17109 Pt. Lena Loop Road, Juneau, AK 99801, USA
[*]corresponding author: lnk.davidson@gmail.com

Abstract

Determining population trends is challenging for marine species with transboundary ranges, but increasingly important given the redistribution of species across international borders with climate change. Here, we use spatiotemporal models fit to data from 10 scientific surveys to evaluate trends in biomass, abundance, and distribution for Pacific Spiny Dogfish (*Squalus suckleyi*) across their entire eastern North Pacific Ocean range. We find a coastwide 51% (95% CI: 38%–61%) decline in Dogfish biomass from 2003–2023. Regional declines were steepest for the US West Coast and Canada: 79% (95% CI: 71%–85%) and 72% (95% CI: 58%–82%), respectively, while Alaskan declines were less steep at 37% (95% CI: 13%–54%). Mature females and immature Dogfish had the largest proportional declines. We find a deepening distribution on the US West Coast and Canada and an increase in the biomass-weighted temperature across most maturity groups on the US West Coast, but these patterns do not explain the overall declines. Contrary to prior hypotheses, we find no clear shift in biomass northward to Alaska. Further work investigating causal mechanisms of the decline is needed.

1 Introduction

Determining population trends can be challenging for wide-ranging, transboundary marine species (Mccauley et al. 2015, Kyne et al. 2020). Survey data for such species may be collected by multiple agencies and by distinct scientific surveys following separate protocols (Maureaud et al. 2021). Population assessments by government agencies tend to focus on regional data with limited communication with nearby agencies. While such regional stock assessments provide important information on local population size and trends, a broader perspective can be valuable for transboundary species—particularly with climate change driving the redistribution of species across international borders and scientific surveys (Maureaud et al. 2021, O'Leary et al. 2021).

The Pacific Spiny Dogfish (*Squalus suckleyi*, hereafter "Dogfish") is an example of a marine species with a wide-ranging, transboundary distribution. In the eastern North Pacific, Dogfish

inhabit waters from Baja California to the Bering Sea (Ketchen 1986) and are commonly found from Oregon to the Gulf of Alaska (Ketchen 1986, Orlov et al. 2012, Gasper and Kruse 2013). Inference on population trends for Dogfish is limited as most scientific surveys have neither the temporal nor spatial coverage to match their slow life history, long lifespan (maximum age around 80–85 years) or their wide-ranging distribution (Mcfarlane and King 2009, Tribuzio and Kruse 2012, Taylor et al. 2013, Gasper and Kruse 2013). Stock assessments estimate regional population trends from local surveys and it is unclear if trends in one region represent the population as a whole or whether local trends could be due to movement to neighbouring regions or changes in frequency of occurrence by size and sex due to their complex size- and sex-specific movements and aggregations.

While Dogfish populations have previously been considered stable and their extinction risk low across the eastern North Pacific coast, (Bigman 2013, Galluci et al. 2011), there is evidence of regional differences underlying this broader assumed stability. In the Canadian portion of their range, uncertainty regarding the abundance of mature females, combined with the species' biological characteristics such as low fecundity, long generation time and gestation period, and vulnerability to overfishing led to an extinction risk categorization of "Special Concern" (COSEWIC 2011). More recently, a stock assessment for Dogfish in British Columbia, Canada (BC) estimated that by the year 2000, unfished spawning output of Dogfish was between 10–40% of unfished levels and total biomass at ≈ 30% of unfished levels (Anderson et al. 2024a). Since then, steep declines in Dogfish biomass were observed in fisheries-independent survey indices in BC (Anderson et al. 2024a, 2019, Anderson and English 2022). On the United States (US) West Coast (the outside waters of Washington, Oregon, and California), the Dogfish population was estimated to be relatively stable in recent years; however, the population was estimated to be at 34% of unfished levels by 2021 and thus above overfished thresholds but below management targets (Gertseva et al. 2021). On the other hand, Dogfish population trends in Alaska are reported to be stable or increasing based on commercial and survey catch rates (Conrath and Foy 2009, Tribuzio and Kruse 2011, Tribuzio et al. 2022). Most changes in regional population size have been suggested to be driven by climate-related movements of individuals outside of each region (Conrath and Foy 2009, Orlov et al. 2012, Gertseva et al. 2021, Shiffman et al. 2022).

Using novel spatiotemporal modelling methods to combine fishery-independent surveys spanning multiple jurisdictions may overcome previous analysis limitations and provide insight on regional and coastwide population trends, distribution, and hotspots of change (e.g., Maureaud et al. 2021, O'Leary et al. 2021, 2022). Here, we use such an approach to ask (1) What is the California to Gulf of Alaska coastwide population trend for Dogfish over the last two decades? (2) How consistent are these trends across regions and might region-specific trends reflect a climate-driven range shift? (3) How consistent are these trends across maturity groups and sexes? (4) What does the distribution of Dogfish by maturity and sex look like along the eastern North Pacific coast and where are hotspots of population density change? (5) Is the depth and temperature distribution of Dogfish stable through time?

Our findings reveal declines along most of the coast with particularly steep declines in British Columbia and the US West Coast; declines across all maturity groups and sexes with the steepest declines in immature and mature female Dogfish; hotspots of decline in southeastern Alaska, off southern Vancouver Island and northern Washington State, and northern Washington; and a general deepening of Dogfish density off British Columbia and the US West Coast, but not in Alaska, potentially suggesting tracking of preferred temperatures in the US West Coast and BC regions.

2 Methods

Broadly, our analytical approach used spatiotemporal models to standardize Dogfish fisheries independent survey data in the eastern North Pacific. We used model predictions to summarize coastwide and regional population trends, population trends by maturity and sex categories, spatially varying local population trends, and to summarize changes to depth distributions. The Supporting

Methods provide a detailed description of data and analytical steps; here we provide a summary of key methodologies.

2.1 Data

We collated data from ten bottom trawl surveys ranging in latitude from California to the Gulf of Alaska that, when considered together, spanned 1980 through to 2023. These data are from three regions: the outside waters of Washington, California, and Oregon (US West Coast) (Keller et al. 2017, Wetzel et al. 2024), British Columbia (BC), Canada (Sinclair et al. 2003, Anderson et al. 2019), and the Gulf of Alaska (GOA), US (NOAA Fisheries 2022, Stauffer 2004). All trawl surveys were conducted with broadly similar gear and collection protocols; however, we tested for differences in survey catchability within our models (Supporting Methods; Figures S12, S13). We obtained longline survey data from the International Pacific Halibut Commission (IPHC) setline survey (IPHC 2022, 2024). These data span 1998–2022, although the survey has not covered the full survey domain in all years (Figure S8).

To model trends in population density and distribution by sex and maturity classes, we split set-level catch weight. Catch weight was split by the proportion of weight from sub-sampled individuals that belonged to each sex and maturity class (immature, maturing, mature). Individuals were assigned to groups using lengths at different probabilities of maturity thresholds (Supporting Methods). As the IPHC survey has only collected Dogfish lengths since 2011, and we were interested in patterns that began in the early 2000s, we focused on the trawl surveys when examining patterns by maturity. In all regions, spatial coverage and collection of lengths has been relatively consistent for trawl surveys since 2003.

2.2 Model structure

To combine fisheries-independent survey data across the eastern North Pacific region of interest, we fit geostatistical generalized linear mixed effects spatiotemporal models. Our full models included quadratic effects for bottom depth, catchability effects, Gaussian Markov random fields (GMRFs) (Rue and Held 2005, Lindgren et al. 2011) accounting for latent spatial effects, and GMRFs structured as random walks to account for latent spatiotemporal effects (Supporting Methods). This model form—although often with independent year means and independent spatiotemporal GMRFs—is a common form of model applied to fish survey data (e.g., Shelton et al. 2014, Thorson et al. 2015, Thorson 2019, Anderson et al. 2024b, Thorson and Kristensen 2024). Given that many of these surveys were conducted biennially or triennially, we used a random walk on the spatiotemporal effects to allow estimation in areas that were not surveyed in some years and to avoid attributing spatial sampling variability to temporal variability. A similar approach was taken in Anderson and English (2022), DFO (2024) and Webster et al. (2020) with the latter using a related first-order autoregressive process.

The coastwide model includes the United States and Canada Pacific coasts (Alaska, British Columbia, Washington, Oregon, and California). The coastwide trawl model spanned 2003–2023 while the coastwide IPHC model spanned 1998–2022. The regional models included (1) Gulf of Alaska, (2) British Columbia, Canada, and (3) Washington, Oregon, California with variable years for trawl (1993–2021, 1984-2023, and 1980–2023 for each region, respectively). The trawl survey catch weight data was fit with Poisson-linked delta-models (Thorson 2018), with a Bernoulli likelihood for encounter/non-encounter of Dogfish, and a (mixture) lognormal likelihood (Thorson et al. 2011) for positive density (accounting for area swept by the trawl net). For most of these models, residual diagnostics (Dunn and Smyth 1996, Smith 1985, Hartig 2022) indicated that a mixture approach was necessary to account for the occasional extreme catch events of Dogfish in trawl surveys (Thorson et al. 2011). We specified a 1% probability that a given positive catch density was drawn from an "extreme" catch distribution—a lognormal distribution with a higher mean but the same dispersion parameter. We fit models to the IPHC count data (as captured Dogfish catch weight

is not recorded) with a negative binomial (NB2; Hilbe 2011) likelihood and a log link with an offset accounting for hooks observed. To determine hotspots of biomass density through time, we fit coastwide models with a spatially varying coefficient of year constrained as a GMRF (Hastie and Tibshirani 1993, Barnett et al. 2021). Some regional and maturity-specific models included fewer encounters and/or less consistent spatial coverage than the full dataset and therefore required simplified model structures (Supporting Methods).

2.3 Parameter estimation

We fit all models with the sdmTMB (Anderson et al. 2024b) R (R Core Team 2024) package, which employs the Stochastic Partial Differential Equation (SPDE) approach (Lindgren et al. 2011) to approximating Gaussian random fields with GMRFs for computational efficiency. sdmTMB uses the fmesher (Lindgren 2023) R package to generate input matrices to carry out SPDE precision matrix calculations, and calculates the marginal log likelihood by integrating over random effects with the Laplace approximation as implemented in the TMB (Kristensen et al. 2016) R package. The negative marginal log likelihood is then minimized via a non-linear minimizer and standard errors on derived quantities of interest are calculated via a generalized delta method (Kristensen et al. 2016).

We conducted a variety of model diagnostics, model comparisons, and assessments of model convergence (Supporting Methods). We compared model structures via the marginal AIC (Akaike information criterion; Akaike 1973) and assessed simulation-based residual diagnostics (Dunn and Smyth 1996, Smith 1985, Hartig 2022, Supporting Methods) to select a model structure. To assess whether our coastwide models generated reasonable representations of the regions, we compared predictions from the coastwide model against those from models fit independently to the regional data. These regional models also provided longer time series, but with more limited spatial coverage and variability in survey timing.

2.4 Calculating population indices and density-weighted depth and temperature

To visualize spatial predictions, calculate area-weighted indices of abundance, and calculate biomass-weighted mean depth occupied, we required a discretized grid covering the domain of the surveys. This allowed for Monte Carlo integration by expanding the variable of interest to each grid cell and calculating a sum across the grid cells (Thorson and Kristensen 2024). We therefore developed 4 km × 4 km and 3 km × 3 km grids that covered the survey domains of the coastwide trawl and longline survey data, respectively (Supporting Methods).

We characterized trends in the trawl and IPHC survey indices two ways. First, for the trawl survey indices of biomass we fit generalized linear models (GLMs) with log links and gamma error to the mean index values by year given the curvilinear declines. We characterize trends for the longline indices using generalized additive models (GAMs) fit with the mgcv R package (Wood 2017), again with log links and gamma error. While we report declines using a log-linear relationship for trawl indices, we acknowledge fluctuations around that trend that mirror patterns in IPHC trends.

We calculated area-weighted indices of relative biomass and abundance by predicting from our spatiotemporal models on the survey grids and summing the product of population density and cell area across the domains. We calculated biomass-weighted mean depth by predicting biomass density for each cell, multiplying the density by cell area to expand to biomass, and taking the biomass-weighted mean depth across grid cells.

3 Results

3.1 Overall population index trends

We observed coastwide declines since the beginning of the coastal time series (2003–2023, Figure 1d) but with variation in magnitude by region (Figure 1e–h). We observed curvilinear declines in Dog-

fish biomass along the entire coast since 2003 (Figure 1c) and GLMs fit to these indices assuming exponential declines characterized average proportional change per decade (Figure 1c). During this time period, the model indicated an average 51% (95% CI: 38%–61%) decline (Figure 1c). Regionally declines were similar on the US West Coast and in BC at 79% (95% CI: 71%–85%) and 72% (95% CI: 58%–82%), respectively; Figure 1c, f, g). The Gulf of Alaska saw a 37% (95% CI: 13%–54%) decline over this time period (Figure 1c, e). The biomass indices generated at the regional level, but using the coastwide spatiotemporal model, were roughly equivalent to those resulting from regional models but with the added advantage of reducing uncertainty and allowing for the estimation of coastwide metrics of interest (Figure 1e, f, g).

Prior to our coastwide trawl model beginning in 2003, regional data suggested varying patterns in biomass indices. In the Gulf of Alaska, surveyed biomass was lower in the 1990s before peaking at 2007 representing a 330% increase in Dogfish biomass during this time (Figure 1e). Dogfish biomass has since declined from this peak and as of 2021 biomass was estimated to be 20% greater than the earliest estimate in 1993 (Figure 1e). In BC, the biomass index prior to 2003 was generated from a survey conducted in a small geographic area of BC's coast (Figure S4). When predicted across BC's coast, this index estimated biomass in BC to be higher than predictions in 2003; however, there is considerable uncertainty since predictions were made across a much larger area than the survey domain (Figure 1f). Estimated biomass trends prior to 2003 on the US West Coast were variable and highly uncertain owing to difference in early surveys, but higher than current estimates (Figure 1g)—fluctuations occurred from lows in the early 1980s and 1995 to the highest estimate in 1997. Except for 2006, every biomass estimate from 2001 onwards is estimated to be below the long-term biomass average (Figure 1g).

Similar to data from trawl surveys, data from the IPHC longline survey also suggest coastwide declines in abundance, albeit less steep (~ 36% decline 1998–2022). Declines were also apparent in BC and on the US West Coast with non-linear patterns through time (Figure 1h–k). The trends across the regions were fairly consistent in their timing, except the Gulf of Alaska increased ~ 40% during the 1998–2003 period while BC and US West Coast declined ~ 50% and 40%, respectively, during this time. The steepest declines in each of the regions were also consistent in magnitude and similar in timing: Gulf of Alaska 67% (2003–2013); BC 65% (2007–2016), and US West Coast 63% (2007–2015) (Figure 1i, j, k). The US West Coast IPHC longline index had a similar decline over the same time-span as the trawl index even though the IPHC survey domain did not include the southern portions of the US West Coast included in the trawl surveys (IPHC survey extended into California in 2013, 2014, and 2017 only) (Figures 1k, S8). Of the IPHC indices, BC had the steepest declines of all of the regions and examined time periods, closely followed by US West Coast. The Gulf of Alaska population did not decline as clearly as the other regions and comprised the majority of Dogfish abundance by 2022, partially attributable to its larger surveyed area (Figure S8).

3.2 Population index trends by maturity

We categorized Dogfish as immature based on a 5% maturity probability cutoff from fitted length-maturity ogives (≤ 65.1 cm males and ≤ 77.0 cm females; Figure 2a, b). All lengths are reported as total length with the tail extended. Immature Dogfish were proportionally encountered more frequently in southern regions than in northern regions (Figure 2c, d). Overall, immature Dogfish formed the largest maturity group by biomass and therefore can be expected to drive the overall patterns in biomass trends (Figure 3a–d). Dogfish categorized as mature females based on a 95% maturity probability (≥ 95.6 cm; Figure 2b, d) generally formed the smallest group by overall biomass (Figure 3a–d). Biomass trends across maturity groups were most synchronous within BC (Figure 3b) and the least synchronous within the US West Coast (Figure 3c).

The steepest overall declines were for Dogfish categorized as mature females in BC with a 72% declines per decade (i.e., proportional decrease of 0.28 per decade; Figure 3d, i), followed by immatures in the US West Coast (70%), maturing females in BC (58%), immatures in Gulf of Alaska (57%) and mature males in BC (56%). Considered together, mature individuals (males and females) declined the greatest in BC (60%), whereas US West Coast and Gulf of Alaska mature individuals

were mostly stable due to the differences in trends between mature females and mature males (Figure 3e, Figure S22). Rates of population decline were similar for immature Dogfish in all regions (Figure 3e, f) with 57%, 56%, and 70% declines per decade (proportional change per decade of 0.43, 0.44, and 0.30), for Gulf of Alaska, BC, and US West Coast, respectively. Similarly, mature females on the US West Coast and BC had similar population index patterns since about 2007 with a spike around 2010 and steep declines of almost 94% and 60% between 2010 and 2021, respectively (Figure 3j). Note the estimate of female biomass between 2009 and 2010 in BC was three times higher from one year to the next. In contrast, increases were only found in mature males in Gulf of Alaska and the US West Coast but the coastwide trend was slightly negative (Figure 3e, g).

3.3 Spatial distribution and trends

By visualizing spatial model predictions from the trawl-survey models for the maturity- and sex-specific groups, we can observe hotspots of Dogfish biomass density (Figure 4a). The waters off the west coast of Vancouver Island and northern Washington State were hotspots of biomass density for all Dogfish maturity groups other than maturing females. Waters in the southeast of the Gulf of Alaska were biomass density hotspots for all groups with the highest biomass density in the deep waters north of Chichagof Island in Alaska (Cross Sound) (Figure S21(iii)). Only immature Dogfish had a hotspot in the southern region of the US West Coast (off Eureka, just south of the Oregon border and north of San Francisco) (Figure S21(v)). There were generally lower densities of Dogfish off the Aleutian Islands, northern BC, and in the waters off southern Washington State, Oregon, and southern California.

Visualizing coefficient estimates from spatially varying trend models illustrates areas of localized population change (Figure 4b). Across all maturity groups, there were coastwide declines with the areas of the greatest decline in Oregon/northern California, Washington/West Coast Vancouver Island, and eastern Alaska. Mature females were the most universally declining group along the entire coast, with almost no areas of increasing biomass density, while immature Dogfish had some of the greatest declines in biomass density (Figure 4b). Maturing males and females also showed declines across the coast; however, with fewer concentrations of steep declines than immature Dogfish. In contrast, mature males had coastwide increases in biomass density with the exception of the area west of Vancouver Island, BC and northern Washington. The waters west of Vancouver Island, BC were a consistent hotspot of estimated biomass density loss with the decline most apparent for immature Dogfish, maturing males, and mature males (Figure 4b). Shelikof Strait, Alaska and the waters around Kodiak Island showed one of the only consistent local increases in biomass, driven by increases in maturing females and mature males, while east of Kodiak Island there were notable declines in all stages, particularly immature and maturing stages (Figure S21(ii)). The US West Coast was similar with hotspots of decline except for mature males and maturing females off California. Estimates of proportional change of biomass per decade (Figure S20b) need to be interpreted in the context of local biomass density from Figure S20a. Six percent of grid cells had a proportional change per decade < 0.2, i.e., a decline $> 80\%$ per decade in the period of 2003–2023 for all maturity groups of Dogfish (Figure S20b). Approximately 11%, 16%, and 11% of grid cells in BC, Gulf of Alaska, and on the US West Coast, respectively, had declines $> 70\%$ per decade after 2003 (Figure S20b).

3.4 Trends in depth and temperature occupied

We observed a decline in biomass-weighted mean depth occupied by Dogfish across most maturity groups in the BC and US West Coast regions but not in the Gulf of Alaska (Figure 5). On the US West Coast, the one group that did not clearly deepen in distribution was mature females. While mature females were initially found at the deepest depths of all the maturity groups (2002) in the US West Coast they were the shallowest maturity group in the other two regions (Figure 5). The deepening of mean depth for Dogfish on the US West Coast for other maturity groups was fairly constant from about 2005 to 2017 but was more variable since then (Figure 5c). The mean depth of Dogfish deepened along a north to south gradient, with stable depths in Alaska and steep depth

profiles in US West Coast, potentially suggestive of Dogfish maintaining their thermal preference across latitudes (Figures 5a–c and d–f).

To understand the potential for shifts in depth to be related to shifts in response to temperature change, the plot of biomass-weighted mean temperature is best interpreted in association with the biomass-weighted depth plot (Figure 5a–c and d–f). We find that the relationship between biomass-weighted mean depth and temperature is variable across regions. While GOA Dogfish depth distribution was mostly stable across maturity groups, the biomass-weighted mean temperature was highly variable and largely tracked the Alaskan temperatures had Dogfish remained stationary (Figure S23a, d). In both BC and the US West Coast, Dogfish maturity group density deepened over time, especially so for the US West Coast populations (Figure 5b, c) While the temperature profile was somewhat consistent for BC (Figure 5b, e), potentially consistent with deepening to track preferred temperatures, the biomass-weighted mean temperature in the US West Coast increased from 2010 onwards (Figure 5c, f).

4 Discussion

Our analysis overcame several challenges with transboundary marine species population species distribution modelling and trend evaluation by combining ten fisheries independent surveys across three regions. This enabled us to evaluate Dogfish from a transboundary perspective and reconcile reports of declines and increases across regional portions of the Dogfish's range. We find that Dogfish have undergone substantial reductions in biomass and numbers over, at least, the past two decades. The coastwide trawl model indicated an average decline steeper than those estimated from the longline coastwide model, perhaps reflecting hyperstability due to the aggregating effect of baiting. We found variability in the regional declines as described by the trawl survey—the US West Coast and BC had similar steep average declines over this time period (79% (95% CI: 71%–85%) and 72% (95% CI: 58%–82%) respectively), while Alaskan declines were less steep (37% (95% CI: 13%–54%)). Although we report exponential changes in relative biomass indices for trawl survey, we note that there are oscillations in the population in both trawl and longline indices. Dogfish categorized as immature both were the largest maturity group by biomass and had the most consistent and largest proportional change per decade in biomass across the regions.

While our analysis provided a transboundary population perspective, we note that our time series is recent and short relative to the life history and exploitation history of this species. Prior to the beginning of our coastwide time series (2003 onwards) the spawning output of Dogfish was estimated to be at 10–30% in BC (Anderson et al. 2024a) Therefore, the population trends and declines we estimated here have occurred on a population that was already depleted.

We find that the recent declines in Dogfish biomass were not obviously explained by movement alone. Determining the causal pathways of the decline requires investigation into prevailing hypotheses including climate-related shifts, overfishing, and predation. A key hypothesis has been that Dogfish shifted their distribution north into Alaska—potentially due to climate change (Conrath and Foy 2009, COSEWIC 2011, Orlov et al. 2012, Gertseva et al. 2021, Shiffman et al. 2022). Indeed, Alaskan (GOA) Dogfish increased between 1993–2007 but are currently estimated to only be 20% greater than 1993 estimates following declines starting around 2003. Despite the long term increase in Alaska, we do not find support for the majority of the declines on the US West Coast or in BC being explained by Dogfish biomass moving north to Alaska. Indices across equivalent time periods in the three regions identified declines and the coastwide trend declined as well. It is possible; however, that there was some northward shift in Dogfish population density resulting in the more gradual decline in the Gulf of Alaska populations.

Additional hypotheses include changes in Dogfish distribution, climate-related changes in preferred depth, and shifts in migration. We find that biomass-weighted depth of Dogfish was deepening in BC and US West Coast, but not Alaska. Here, we were unable to disentangle if this deepening trend represents a shift deeper, a loss of biomass in the shallower depths, or both. If the deepening trend reflects a shift of biomass, we note that the movement to waters deeper than the survey

domain is unlikely to explain the decline. While it is possible that Dogfish have shifted outside of the survey domain, i.e., offshore or inshore into inlets (sensu Barndoor skate *Dipturus laevis* in the Atlantic Simon et al. 2002, Casey and Myers 1998), additional lines of evidence suggest that this has not happened for Dogfish. The trawl surveys already encompass the bulk of Dogfish's depth distribution. Declines in commercial catch per unit effort from the bottom trawl fleet in BC suggest declines occurred throughout the year and across depths (Anderson et al. 2019, 2024a) while a stable trend in the Alaskan deep-water longline survey (C. Tribuzio, pers. comm.) and in a deep-water trap survey in BC (Anderson et al. 2024a) suggests Dogfish have not moved to slope habitat.

Although we did not directly test environmental variables as a predictor of distribution change, our work is consistent with findings from earlier work. Localized changes to Dogfish biomass density off BC were found to be negatively associated with increasing bottom temperature and dissolved oxygen (English et al. 2021). Other recent work has suggested that coastwide Dogfish distribution may contract in warmer years (Ward et al. 2024). Our findings are consistent with Dogfish maintaining a thermal niche by deepening their depth in the more southern parts of their distribution. While GOA Dogfish showed a relatively stationary distribution despite fluctuations in temperature, BC and US West Coast Dogfish showed a deepening and either stable or increasing occupied temperatures. The US West Coast Dogfish deepened while temperatures remained stable or increased. This potentially reflects loss of available habitat or an artifact of the loss of biomass in the northernmost parts of the US West Coast. Regardless, climate-related deepening of the population cannot sufficiently explain declines as there was no evidence of climate tracking in Alaska and Dogfish are not thought to have life histories that are susceptible to climate forcing as they occupy a wide thermal breadth, are equilibrium strategists, and give birth to large live offspring (Wood et al. 1979, King and McFarlane 2003, Yatsu et al. 2008).

Finally, not tested here was a potential for shifts in migration timing. Previous work found that Dogfish shifted their migration timing by a month in Japan (Kanamori et al. 2023). We found that mature females were shallower in recent years in both the US West Coast spring and fall surveys. This potential depth re-distribution by maturity and sex class may suggest a shift to shallower waters but these findings were not consistent across regions.

The main cause of shark, ray, skate, and chimaera (Chondrichthyes) declines globally is overfishing (Dulvy et al. 2021). Given the slow life-history traits of sharks and rays, the signal of past fishing pressure can lag in population trends. For example, the North Atlantic Shortfin Mako (*Isurus oxyrinchus*) stock assessment found that historical fishing pressure selected immature individuals resulting in an initially stable mature population size as mature individuals were not selected. Continued fishing on immature size classes; however, resulted in growth overfishing leading to declines in biomass as older individuals died out (Winker et al. 2020, D. Courtney, pers. comm.). Similarly, the large sex-biased fishery on Atlantic Spiny Dogfish (*Squalus acanthias*) resulted in population trends with oscillations as the higher removals of mature female Dogfish exceeded recruitment of individuals into the mature population. Consequently, the population went through periods of higher and lower recruitment (Rago and Sosebee 2013). A period of low recruitment between 1997–2003 was characterized by a decline in the number of pups being born and a decline in mean length of mature females (Rago and Sosebee 2013). For Pacific Spiny Dogfish, past fishing effort was focused mainly on large females. The large Dogfish liver oil fishery in the 1940s peaked at ~ 50,000 t/year in BC and US West Coast and selected large females as their vitamin A potency was the highest (Barraclough 1948, King et al. 2017). This intense fishing on mature females could have driven long-term oscillations in spawning output due to a subsequent missing cohort of juvenile dogfish (Wood et al. 1979, Anderson et al. 2024a).

Despite lower landings of Dogfish relative to historical levels in the eastern North Pacific, the potential for contemporary overfishing remains due to challenges in developing stock assessment advice, continued high incidental catches, and discard mortality. Traditional stock assessments are difficult for Dogfish for several reasons. For example, Dogfish are difficult to age (Mcfarlane and King 2009), Dogfish are a transboundary stock with the highest population density at an international border between Washington and BC with seasonal migration across the border (Gertseva et al. 2021, Taylor et al. 2013, Taylor 2008), and population indices for Dogfish are not available

during the early intense phases of their fishing history nearly a century ago. These issues introduce considerable challenges for regional stock assessments. Despite these challenges, a recent stock assessment in BC found that overfishing may have occurred from the 1980s through to about 2010, which may have coincided with a decline in spawning output due to a legacy effect from the intense fishing of the 1940s (Anderson et al. 2024a). On the US West Coast, overfishing may also have occurred in the 1980s and early 2000s (Gertseva et al. 2021). While the current target reference point is associated with a spawning potential ratio of 50% for the US West Coast population, this harvest control rule is under revision as the life history of Dogfish may require more conservative targets (Gertseva et al. 2021).

While Dogfish are generally thought of as predators, they are also prey, and prey switching, ecosystem changes, or predator pits (where prey populations can be held at low densities due to even low amounts of predation, e.g., Swain and Benoît 2015), are all potential causes of their ongoing declines. Here, we find the steepest declines in Dogfish biomass were at shallower depths and driven by declines in juvenile biomass. One possible source of predation is from Steller Sea Lions (*Eumetopias jubatus*) and/or California Sea Lions (*Zalophus californianus*). Across the coast, Steller Sea Lion and California Sea Lion populations have increased in recent decades with regional variation in the magnitude of the increase. In BC, the Steller Sea Lion population increased from historic lows to numbers greater than population estimates from the early 1900s and the California Sea Lion population has nearly tripled since 2010 (DFO 2020, 2023). On the US West Coast, California Sea Lions population numbers levelled off in 2014 after 30–40 years of increase (Lowry et al. 2022) while Steller Sea Lions have continued to increase steadily since 1975 (Laake et al. 2018). Alaskan Steller Sea Lion populations declined during the 1990s in the eastern portion of their range but between 2000–2004 the western population was stable and the eastern population increased (Trites et al. 2007). Additional sources of predation mortality could include Offshore Killer Whales (*Orcinus orca*), which consume sharks as part of their diet (DFO 2018). With the steep population decline of Offshore Killer Whales' potential preferred prey, Basking sharks (*Cetorhinus maximus*) (DFO 2018), increased reliance on Dogfish is a possibility. While predation may have remained static through time, predation may have differential impacts on a heavily depleted versus a less-depleted population.

Many sharks and rays are threatened with extinction due to their slow life history, late age of maturity, long gestation, and low fecundity (Dulvy et al. 2021). Population changes of marine species can be challenging to detect and especially so for wide-ranging, transboundary species where data may be collected by multiple surveys across multiple jurisdictions. Combining fisheries-independent survey data permitted the evaluation of transboundary population size changes while also highlighting that regional declines are not obviously due to northward movements outside of each region.

From a conservation perspective, Dogfish have long been considered a nuisance species of low management and conservation concern (Mcfarlane and King 2002) and are currently not a high-valued commercial fish. Their role in the ecosystem is not well understood. They are not a high-level predator but could potentially have impacts on or influence other species via predation and nutrient transfer due to their population size and relatively ubiquitous distribution in the eastern North Pacific. Although historically abundant and once valued, evidence suggests that Dogfish now could be categorized with a higher extinction risk both regionally and coastwide.

5 Acknowledgements

We thank Fisheries and Oceans Canada's Species at Risk Program (SARP) and Competitive Science Research Fund (CSRF) for funding that supported this work. We thank the Groundfish surveys teams (M.R. Wyeth, Norm Olsen, Kristina Castle, Schon Hardy, Katherine Temple), the Data unit (Maria Cornthwaite and Jonathon Faris), the Coast Guard Crew on the Neocaligus and Franklin past and present and the US surveys teams and crew. We thank E.J. Ward and S.A. Pardo for comments that improved this manuscript.

Data availability: Code and data to replicate the analyses in this paper are available at https://github.com/pbs-assess/dogfish-trends and will be archived at Zenodo prior to publication.

References

Aitchison, J. 1955. On the distribution of a positive random variable having a discrete probability mass at the origin. Journal of the American Statistical Association **50**(271): 901. doi:10.2307/2281175.

Akaike, H. 1973. Information theory as an extension of the maximum likelihood principle. In Second International Symposium on Information Theory, Akademiai Kiado, Budapest, pp. 267–281.

Anderson, S.C. and English, P.A. 2022. Trends in Pacific Canadian groundfish stock status. In State of the Physical, Biological and Selected Fishery Resources of Pacific Canadian Marine Ecosystems in 2021. Eds. J. Boldt, E. Joyce, S. Tucker, S. Gauthier. Can. Tech. Rep. Fish. Aquat. Sci. **3482**: 112–120. https://www.dfo-mpo.gc.ca/oceans/publications/soto-rceo/2021/technical-report-rapport-technique-eng.html.

Anderson, S.C., Keppel, E.A., and Edwards, A.M. 2019. A reproducible data synopsis for over 100 species of British Columbia groundfish. DFO Can. Sci. Advis. Sec. Res. Doc. **2019/041**: vii + 321 p.

Anderson, S.C., Huynh, Q.C., Davidson, L.N., and King, J.R. 2024a. Pacific Spiny Dogfish (*Squalus suckleyi*) population modelling for outside waters of British Columbia 2024. DFO Can. Sci. Advis. Sec. Res. Doc. **In press**: v + 168 p.

Anderson, S.C., Ward, E.J., English, P.A., Barnett, L.A.K., and Thorson, J.T. 2024b. sdmTMB: An R package for fast, flexible, and user-friendly generalized linear mixed effects models with spatial and spatiotemporal random fields. bioRxiv **2022.03.24.485545**. doi:10.1101/2022.03.24.485545.

Andrews, K.S. and Harvey, C.J. 2013. Ecosystem-level consequences of movement: Seasonal variation in the trophic impact of a top predator. Marine Ecology Progress Series **473**: 247–260. doi:10.3354/meps10095.

Barnett, L.A.K., Ward, E.J., and Anderson, S.C. 2021. Improving estimates of species distribution change by incorporating local trends. Ecography **44**(3): 427–439. doi:10.1111/ecog.05176.

Barraclough, W.E. 1948. The sunken gill-net fishery, and an analysis of the availability of the dog-fish (*Squalus suckleyi* Girard) and the soup-fin shark (*Galeohinus galeus* Linnaeus) in British Columbia waters from 1943-1946. Ph.D. thesis, The University of British Columbia.

Bigman, J.S. 2013. Trophic ecology of north pacific spiny dogfish (*Squalus suckleyi*) off Central California waters. Master's thesis, California State University.

Casey, J.M. and Myers, R.A. 1998. Near extinction of a large, widely distributed fish. Science **281**(5377): 690–692. doi:10.1126/science.281.5377.690.

Conrath, C.L. and Foy, R.J. 2009. A History of the Distribution and Abundance of Spiny Dogfish in Alaska Waters. In Biology and Management of Dogfish Sharks, edited by G.G. Gallucci, Vincent F., McFarlane, G.A., Bargmann, American Fisheries Society, Bethesda, Maryland, pp. 119–126.

COSEWIC 2011. COSEWIC assessment and status resport on the North Pacific Spiny Dogfish *Squalus suckleyi* in Canada. Technical report, Ottawa.

DFO 2018. Recovery strategy for the offshore killer whales (*Orcinus orca*) in Canada [Proposed]. Technical report, Fisheries and Oceans Canada, Ottawa.

DFO 2020. Status of Steller Sea Lions (*Eumetopias jubatus*) in Canada. DFO Canadian Science Advisory Secretariat Science Advisory Report. 2020/046 (October): 13.

DFO 2023. Groundfish Integrated Fisheries Management Plan 2023/24.

DFO 2024. Application of the management procedure framework for inside Quillback Rockfish (*sebastes maliger*) in British Columbia in 2022. DFO Can. Sci. Advis. Sec. Sci. Advis. Rep. **2024/017**.

Dulvy, N.K., Pacoureau, N., Rigby, C.L., Pollom, R.A., Jabado, R.W., Ebert, D.A., Finucci, B., Pollock, C.M., Cheok, J., Derrick, D.H., Herman, K.B., Sherman, C.S., VanderWright, W.J., Lawson, J.M., Walls, R.H., Carlson, J.K., Charvet, P., Bineesh, K.K., Fernando, D., Ralph, G.M., Matsushiba, J.H., Hilton-Taylor, C., Fordham, S.V., and Simpfendorfer, C.A. 2021. Overfishing drives over one-third of all sharks and rays toward a global extinction crisis. Current Biology **31**(21): 4773–4787.e8. doi: 10.1016/j.cub.2021.08.062.

Dunn, P.K. and Smyth, G.K. 1996. Randomized Quantile Residuals. Journal of Computational and Graphical Statistics **5**(3): 236–244. doi:10.1080/10618600.1996.10474708.

Edwards, A.M., Anderson, S.C., Keppel, E.A., and Grandin, C.J. 2023. gfiphc: Data Extraction and Analysis for Groundfish Data from the IPHC Longline Survey in BC. R package version 1.2.0.

English, P.A., Ward, E.J., Rooper, C.N., Forrest, R.E., Rogers, L.A., Hunter, K.L., Edwards, A.M., Connors, B.M., and Anderson, S.C. 2021. Contrasting climate velocity impacts in warm and cool locations show that effects of marine warming are worse in already warmer temperate waters. Fish and Fisheries **23**(1): 239–255. doi:10.1111/faf.12613.

Fuglstad, G.A., Simpson, D., Lindgren, F., and Rue, H. 2015. Constructing priors that penalize the complexity of Gaussian random fields. arXiv:1503.00256 [stat] .

Galluci, V., Taylor, I., King, J., McFarlane, G., and McPhie, R. 2011. Spiny dogfish (*Squalus acanthias*) assessment and catch recommendations for 2010. DFO Can. Sci. Advis. Sec. Res. Doc. 2011/034. pp. 1–69.

Gasper, J.R. and Kruse, G.H. 2013. Modeling of the spatial distribution of Pacific spiny dogfish (Squalus suckleyi) in the Gulf of Alaska using generalized additive and generalized linear models. Canadian Journal of Fisheries and Aquatic Sciences **70**(9): 1372–1385. doi:10.1139/cjfas-2012-0535.

Gertseva, V., Taylor, I., Wallace, J., and Matson, S.E. 2021. Status of the Pacific Spiny Dogfish shark resource off the continental U.S. Pacific Coast in 2021. Technical report.

Hartig, F. 2022. DHARMa: Residual Diagnostics for Hierarchical (Multi-Level/Mixed) Regression Models. R package version 0.4.6.

Hastie, T. and Tibshirani, R. 1993. Varying-Coefficient Models. Journal of the Royal Statistical Society. Series B (Methodological) **55**(4): 757–796.

Hilbe, J.M. 2011. Negative Binomial Regression. Cambridge University Press.

IPHC 2022. Fisheries Independent Setline Survey FISS .

IPHC 2024. IPHC Fishery-Independent Setline Survey Sampling Manual (2024). IPHC–2024–VSM01 pp. 1–39.

Kanamori, Y., Yano, T., Okamura, H., and Yagi, Y. 2023. Spatio-temporal model and machine learning method reveal patterns and processes of migration under climate change. Journal of Biogeography (February): 1–11. doi:10.1111/jbi.14595.

Keller, A.A., Wallace, J.R., and Methot, R.D. 2017. The Northwest Fisheries Science Center's West Coast Groundfish Bottom Trawl Survey : history, design, and description. Technical report, North West Fisheries Science Center.

Keppel, E.A., S.A.A.E. and Grandin, C. 2022. gfdata: Data Extraction for DFO PBS Groundfish Stocks. R package version 0.0.0.9000.

Ketchen, K.S. 1986. The spiny dogfish (*Squalus acanthias*) in the northeast Pacific and a history of its utilization. Dept. of Fisheries and Oceans.

King, J., McFarlane, G.A., Gertseva, V., Gasper, J., Matson, S., and Tribuzio, C.A. 2017. Shark Interactions With Directed and Incidental Fisheries in the Northeast Pacific Ocean: Historic and Current Encounters, and Challenges for Shark Conservation, volume 78. Elsevier Ltd., 1 edition. doi:10.1016/bs.amb.2017.09.003.

King, J.R. and McFarlane, G.A. 2003. Marine fish life history strategies: Applications to fishery management. Fisheries Management and Ecology **10**(4): 249–264. doi:10.1046/j.1365-2400.2003.00359.x.

Kristensen, K., Nielsen, A., Berg, C.W., Skaug, H., and Bell, B.M. 2016. TMB: Automatic differentiation and Laplace approximation. Journal of Statistical Software **70**(5): 1–21. doi:10.18637/jss.v070.i05.

Kyne, P.M., Gore, M.A., Ebert, D.A., Jabado, R.W., Rigby, C.L., Pollock, C.M., Herman, K.B., Simpfendorfer, C.A., Cheok, J., and Dulvy, N.K. 2020. The thin edge of the wedge : Extremely high extinction risk in wedgefishes and giant guitarfishes (February): 1–25. doi:10.1002/aqc.3331.

Laake, J.L., Lowry, M.S., DeLong, R.L., Melin, S.R., and Carretta, J.V. 2018. Population growth and status of california sea lions. Journal of Wildlife Management **82**(3): 583–595. doi:10.1002/jwmg.21405.

Lindgren, F. 2023. fmesher: Triangle Meshes and Related Geometry Tools. R package version 0.1.5.

Lindgren, F., Rue, H., and Lindström, J. 2011. An explicit link between Gaussian fields and Gaussian Markov random fields: The stochastic partial differential equation approach. Journal of the Royal Statistical Society: Series B (Statistical Methodology) **73**(4): 423–498. doi:10.1111/j.1467-9868.2011.00777.x.

Lowry, M.S., Nehasil, S.E., and Moore, J.E. 2022. Spatio-temporal diet variability of the California sea lion Zalophus californianus in the southern California Current Ecosystem. Marine Ecology Progress Series **692**: 1–21. doi:10.3354/meps14096.

Maureaud, A.A., Frelat, R., Pécuchet, L., Shackell, N., Mérigot, B., Pinsky, M.L., Amador, K., Anderson, S.C., Arkhipkin, A., Auber, A., Barri, I., Bell, R.J., Belmaker, J., Beukhof, E., Camara, M.L., Guevara-Carrasco, R., Choi, J., Christensen, H.T., Conner, J., Cubillos, L.A., Diadhiou, H.D., Edelist, D., Emblemsvåg, M., Ernst, B., Fairweather, T.P., Fock, H.O., Friedland, K.D., Garcia, C.B., Gascuel, D., Gislason, H., Goren, M., Guitton, J., Jouffre, D., Hattab, T., Hidalgo, M., Kathena, J.N., Knuckey, I., Kidé, S.O., Koen-Alonso, M., Koopman, M., Kulik, V., León, J.P., Levitt-Barmats, Y., Lindegren, M., Llope, M., Massiot-Granier, F., Masski, H., McLean, M., Meissa, B., Mérillet, L., Mihneva, V., Nunoo, F.K.E., O'Driscoll, R., O'Leary, C.A., Petrova, E., Ramos, J.E., Refes, W., Román-Marcote, E., Siegstad, H., Sobrino, I., Sólmundsson, J., Sonin, O., Spies, I., Steingrund, P., Stephenson, F., Stern, N., Tserkova, F., Tserpes, G., Tzanatos, E., van Rijn, I., van Zwieten, P.A.M., Vasilakopoulos, P., Yepsen, D.V., Ziegler, P., and Thorson, J.T. 2021. Are we ready to track climate-driven shifts in marine species across international boundaries? - A global survey of scientific bottom trawl data. Global Change Biology **27**(2): 220–236. doi:10.1111/gcb.15404.

Mccauley, D.J., Pinsky, M.L., Palumbi, S.R., Estes, J.A., Joyce, F.H., and Warner, R.R. 2015. The global ocean **347**(6219). doi:10.1126/science.1255641.

Mcfarlane, G.A. and King, J. 2009. Re-evaluating the age determination of spiny dogfish using oxytetracycline and fish at liberty up to 20 years. In Biology and Management of Dogfish Sharks, edited by V.F. Gallucci, M.G. A., and G.G. Bargmann, American Fisheries Society, Bethesda, Maryland, USA, pp. 153–160.

Mcfarlane, G.A. and King, J.R. 2002. Migration patterns of Spiny Dogfish (Squalus acanthias) in the North Pacific Ocean. Fisheries Bulletin **2**(101): 358–367.

NOAA Fisheries 2022. Fisheries One Stop Shop FOSS .

O'Leary, C.A., Kotwicki, S., Hoff, G.R., Thorson, J.T., Kulik, V.V., Ianelli, J.N., Lauth, R.R., Nichol, D.G., Conner, J., and Punt, A.E. 2021. Estimating spatiotemporal availability of transboundary fishes to fishery-independent surveys. Journal of Applied Ecology **58**(10): 2146–2157. doi:10.1111/1365-2664.13914.

O'Leary, C.A., DeFilippo, L.B., Thorson, J.T., Kotwicki, S., Hoff, G.R., Kulik, V.V., Ianelli, J.N., and Punt, A.E. 2022. Understanding transboundary stocks' availability by combining multiple fisheries-independent surveys and oceanographic conditions in spatiotemporal models. ICES Journal of Marine Science p. fsac046. doi:10.1093/icesjms/fsac046.

Orlov, A.M., Savinykh, V.F., Kulish, E.F., and Pelenev, D.V. 2012. New data on the distribution and size composition of the North Pacific spiny dgofish *Squalus suckelyi* (Girard, 1854). Scientia Marina **76**(1): 111–122. doi:10.3989/scimar.03439.22C.

Pante, E., Simon-Bouhet, B., and Irisson, J.O. 2023. marmap: Import, Plot and Analyze Bathymetric and Topographic Data. R package version 1.0.10.

R Core Team 2024. R: A Language and Environment for Statistical Computing. R Foundation for Statistical Computing, Vienna, Austria.

Rago, P. and Sosebee, K. 2013. Update on the Status of Spiny Dogfish in 2013 and projected harvests at the Fmsy Proxy and Pstar of 40 Report to the Mid Atlantic Fishery Management Council Scientific and Statistical Committee pp. 1–51.

Rue, H. and Held, L. 2005. Gaussian Markov Random Fields: Theory and Applications. CRC press.

Shelton, A.O., Thorson, J.T., Ward, E.J., and Feist, B.E. 2014. Spatial semiparametric models improve estimates of species abundance and distribution. Canadian Journal of Fisheries and Aquatic Sciences **71**(11): 1655–1666. doi:10.1139/cjfas-2013-0508.

Shiffman, D., Bangley, C., and Macdonald, C. 2022. "A prized Pacific shark": the rise and fall (and rise again..?) of the world's first ecolabel certified sustainable shark fishery. Fish Biology **103**(3): 623–634. doi:10.1111/jfb.15467.

Simon, J.E., Frank, K.T., and Kulka, D.W. 2002. Distribution and abundance of barndoor skate Dipturus laevis in the Canadian Atlantic based upon research vessel surveys and industry/science surveys. Research Document p. 68.

Sinclair, A., Schnute, J., Haigh, R., Starr, P., Stanley, R., Fargo, J., and Workman, G. 2003. Feasibility of multispecies groundfish trawl surveys on the BC coast. DFO Can. Sci. Adv. Sec. Res. Doc. **2003/049**: i + 34 p.

Smith, J.Q. 1985. Diagnostic checks of non-standard time series models. Journal of Forecasting **4**(3): 283–291. doi:10.1002/for.3980040305.

Stauffer, G. 2004. NOAA protocols for groundfish bottom trawl surveys of the nation's fishery resources. Technical Report NOAA Tech. Memo., U.S. Dep. Commer.

Swain, D.P. and Benoît, H.P. 2015. Extreme increases in natural mortality prevent recovery of collapsed fish populations in a Northwest Atlantic ecosystem **519**: 165–182. doi:10.3354/meps11012.

Taylor, I.G. 2008. Modeling spiny dogfish population dynamics in the Northeast Pacific. Ph.D. thesis, University of Washington.

Taylor, I.G., Gertseva, V., and Matson, S.E. 2013. Spine-based ageing methods in the spiny dogfish shark, *Squalus suckleyi*: How they measure up. Fisheries Research **147**: 83–92. doi:10.1016/j.fishres.2013.04.011.

Thorson, J.T. 2018. Three problems with the conventional delta-model for biomass sampling data, and a computationally efficient alternative. Canadian Journal of Fisheries and Aquatic Sciences **75**(9): 1369–1382. doi:10.1139/cjfas-2017-0266.

Thorson, J.T. 2019. Guidance for decisions using the Vector Autoregressive Spatio-Temporal (VAST) package in stock, ecosystem, habitat and climate assessments. Fisheries Research **210**: 143–161. doi:10.1016/j.fishres.2018.10.013.

Thorson, J.T. and Kristensen, K. 2016. Implementing a generic method for bias correction in statistical models using random effects, with spatial and population dynamics examples. Fisheries Research **175**: 66–74. doi:10.1016/j.fishres.2015.11.016.

Thorson, J.T. and Kristensen, K. 2024. Spatio-Temporal Models for Ecologists. CRC Press, Boca Raton, FL.

Thorson, J.T., Stewart, I.J., and Punt, A.E. 2011. Accounting for fish shoals in single- and multi-species survey data using mixture distribution models. Canadian Journal of Fisheries and Aquatic Sciences **68**(9): 1681–1693. doi:10.1139/F2011-086.

Thorson, J.T., Shelton, A.O., Ward, E.J., and Skaug, H.J. 2015. Geostatistical delta-generalized linear mixed models improve precision for estimated abundance indices for West Coast groundfishes. ICES J. Mar. Sci. **72**(5): 1297–1310. doi:10.1093/icesjms/fsu243.

Thygesen, U.H., Albertsen, C.M., Berg, C.W., Kristensen, K., and Nielsen, A. 2017. Validation of ecological state space models using the Laplace approximation. Environmental and Ecological Statistics **24**(2): 317–339. doi:10.1007/s10651-017-0372-4.

Tribuzio, C.A. and Kruse, G.H. 2011. Demographic and risk analyses of spiny dogfish (*Squalus suckleyi*) in the Gulf of Alaska using age- and stage-based population models. Marine and Freshwater Research **62**(12): 1395–1406. doi:10.1071/MF11062.

Tribuzio, C.A. and Kruse, G.H. 2012. Life history characteristics of a lightly exploited stock of *Squalus suckleyi*. Journal of Fish Biology **80**(5): 1159–1180. doi:10.1111/j.1095-8649.2012.03241.x.

Tribuzio, C.A., Gallucci, V.F., and Bargmann, G.G. 2009. 6. Reproductive Biology and Management Implications for Spiny Dogfish in Puget Sound, Washington. Technical report.

Tribuzio, C.A., Matta, M.E., Echave, K.B., Rodgveller, C., Dunne, G., and Fuller, K. 2022. 9. Assessment of the Shark Stock Complex in the Bering Sea/Aleutian Islands and Gulf of Alaska (December 2022).

Trites, A.W., Miller, A.J., Maschner, H.D., Alexander, M.A., Bograd, S.J., Calder, J.A., Capotondi, A., Coyle, K.O., Lorenzo, E.D., Finney, B.P., Gregr, E.J., Grosch, C.E., Hare, S.R., Hunt, G.L., Jahncke, J., Kachel, N.B., Kim, H.J., Ladd, C., Mantua, N.J., Marzban, C., Maslowski, W., Mendelssohn, R., Neilson, D.J., Okkonen, S.R., Overland, J.E., Reedy-Maschner, K.L., Royer, T.C., Schwing, F.B., Wang, J.X., and Winship, A.J. 2007. Bottom-up forcing and the decline of Steller sea lions (Eumetopias jubatas) in Alaska: Assessing the ocean climate hypothesis. Fisheries Oceanography **16**(1): 46–67. doi:10.1111/j.1365-2419.2006.00408.x.

Tweedie, M.C.K. 1984. An index which distinguishes between some important exponential families. In Statistics: Applications and New Directions. Proceedings of the Indian Statistical Institute Golden Jubilee International Conference, edited by J.K. Gosh and J. Roy, Indian Statistical Institute, Calcutta, pp. 579–604.

Waagepetersen, R. 2006. A Simulation-Based Goodness-of-Fit Test for Random Effects in Generalized Linear Mixed Models. Scandinavian Journal of Statistics **33**(4): 721–731.

Ward, E.J., Anderson, S.C., Barnett, L.A.K., Ferriss, B.E., Rooper, C., Wetzel, C.R., Johnson, K.F., Whitmire, C.E., English, P.A., and Thorson, J.T. 2023. surveyjoin: Combine Data from Northeast Pacific Ocean Fish Surveys. R package version 0.0.1.

Ward, E.J., Anderson, S.C., Barnett, L.A.K., English, P.A., Berger, H.M., Commander, C.J.C., Essington, T.E., Harvey, J., Hunsicker, M.E., Jacox, M.G., Johnson, K.F., Large, S., Liu, O.R., Richerson, K.E., Samhour, J.F., Siedlecki, A., Shelton, A.O., Somers, K.A., and Watson, J.T. 2024. Win, lose, or draw: Evaluating dynamic thermal niches of northeast Pacific groundfish. PLOS Climate **3**(11): 1–19. doi:10.1371/journal.pclm.0000454.

Webster, R.A., Soderlund, E., Dykstra, C.L., and Stewart, I.J. 2020. Monitoring change in a dynamic environment: Spatiotemporal modelling of calibrated data from different types of fisheries surveys of pacific halibut. Canadian Journal of Fisheries and Aquatic Sciences **77**(8): 1421–1432. doi:10.1139/cjfas-2019-0240.

Wetzel, C.R., Johnson, K.F., and Hicks, A.C. 2024. nwfscSurvey: Northwest Fisheries Science Center Survey. R package version 2.1.

Winker, H., Carvalho, F., and Kerwath, S. 2020. Age-structured biomass dynamics of north Atlantic shortfin mako with implications for the interpretation of surplus production models. Collective Volume of Scientific Papers ICCAT **76**(10): 316–336.

Wood, C.C., Ketchen, K.S., and Beamish, R.J. 1979. Population Dynamics of Spiny Dogfish (*Squalus acanthias*) in British Columbia Waters. Journal of the Fisheries Research Board of Canada **36**(6): 647–656. doi:10.1139/f79-094.

Wood, S. 2017. Generalized Additive Models: An Introduction with R. Chapman and Hall/CRC, 2 edition.

Wyeth, M. 2024. Summary of the Fisheries and Oceans, Canada Pacific Region Groundfish Fishing Survey Program in 2022. Technical report, Department of Fisheries and Oceans, Nanaimo, BC.

Wyeth, M.R., Olsen, N., Nottingham, M.K., and Williams, D.C. 2018. Summary of the Hecate Strait synoptic bottom trawl survey, May 26 – June 22, 2015. DFO Can. Manuscr. Rep. Fish. Aquat. Sci. **2018/3126**: viii + 55 p.

Yatsu, A., Aydin, K.Y., King, J.R., McFarlane, G.A., Chiba, S., Tadokoro, K., Kaeriyama, M., and Watanabe, Y. 2008. Elucidating dynamic responses of North Pacific fish populations to climatic forcing: Influence of life-history strategy. Progress in Oceanography **77**(2-3): 252–268. doi:10.1016/j.pocean.2008.03.009.

6 Figures

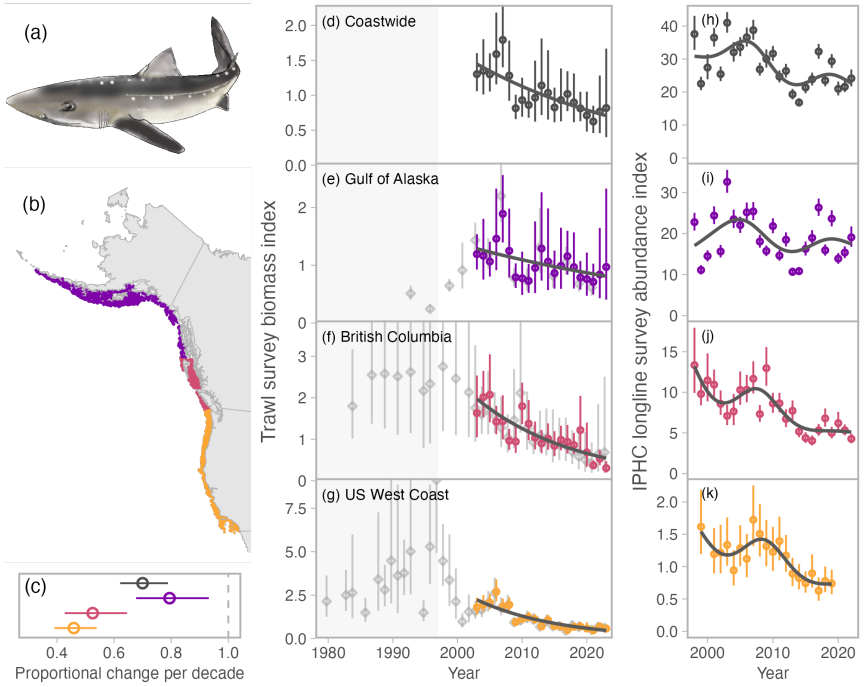

Figure 1: Trends in population density of Dogfish across the eastern North Pacific coast from the Gulf of Alaska to California. (a) Drawing of a Pacific Spiny Dogfish. (b) Distribution of fisheries independent trawl survey data and regions of interest. (c) Slope coefficients describing the multiplicative population change per decade from 2003 onwards for the trawl surveys. (d–g) Standardized and normalized population trends coastwide and by region from trawl surveys. Grey diamonds represent estimates from regional models; coloured circles represent estimates from a coastwide model. Fitted lines represent log-linked generalized linear models with gamma error fit to the coastwide model trends from 2003 onwards (slopes shown in panel c). All time series are normalized to have a geometric mean of 1 for 2003–2022. Grey shading indicates the time period prior to the start date of the IPHC longline survey. (h–k) Standardized relative abundance from the IPHC longline survey for the same regions as for trawl. Fitted lines represents a log-linked generalized additive model with gamma error. Throughout, dots and line segments represent means and 95% confidence intervals, respectively. Dogfish drawing created by Edith Kraus and used with permission.

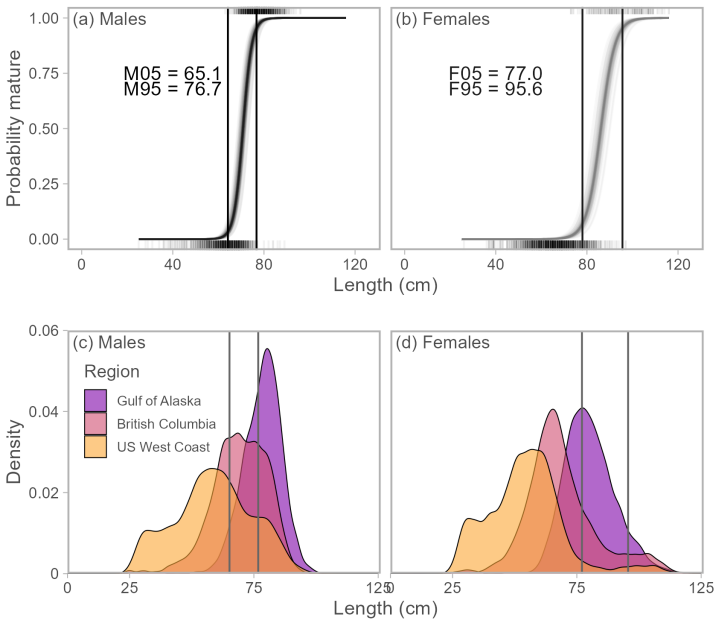

Figure 2: Maturity definitions and distribution of lengths captured by trawl surveys. Maturity ogives for (a) male and (b) female Dogfish with estimated lengths at maturity. Individual curved lines represent ogives by sample ID, which was treated as a random intercept in a GLMM with a logit link and Bernoulli error. Density plots of captured Dogfish within regional trawl surveys for (c) males and (d) females. Vertical lines indicate lengths at 0.05 and 0.95 probability of maturity. Dogfish below the 0.05 threshold were considered "immature". Dogfish between 0.05 and 0.95 were considered "maturing". Dogfish greater than the 0.95 threshold were considered "mature". Length was measured with tail extended.

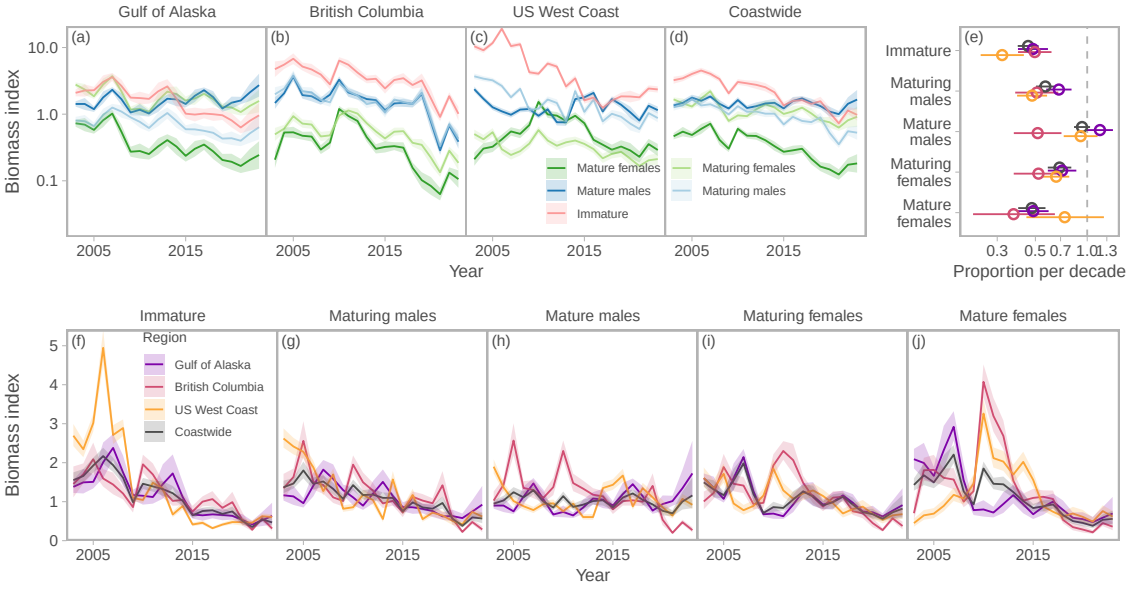

Figure 3: Relative biomass trends by maturity group and region. (a–d) Biomass indices coloured by maturity group and arranged in panels by region and then all regions combined (d–coastwide). Each panel has a geometric mean of 1 and the y-axis here is log-distributed. (e) Proportional change in biomass per decade from 2003 onwards from a log-linked GLM with gamma error. (f–j) Biomass indices coloured by region and arranged in panels by maturity group. Each time series is scaled to have a geometric mean of 1 to assess synchrony within maturity groups across regions. Lines and ribbons in panels a–d and f–j represent means and 50% confidence intervals (to minimize visual overlap), respectively. Dots and lines in panel e represent means and 95% confidence intervals.

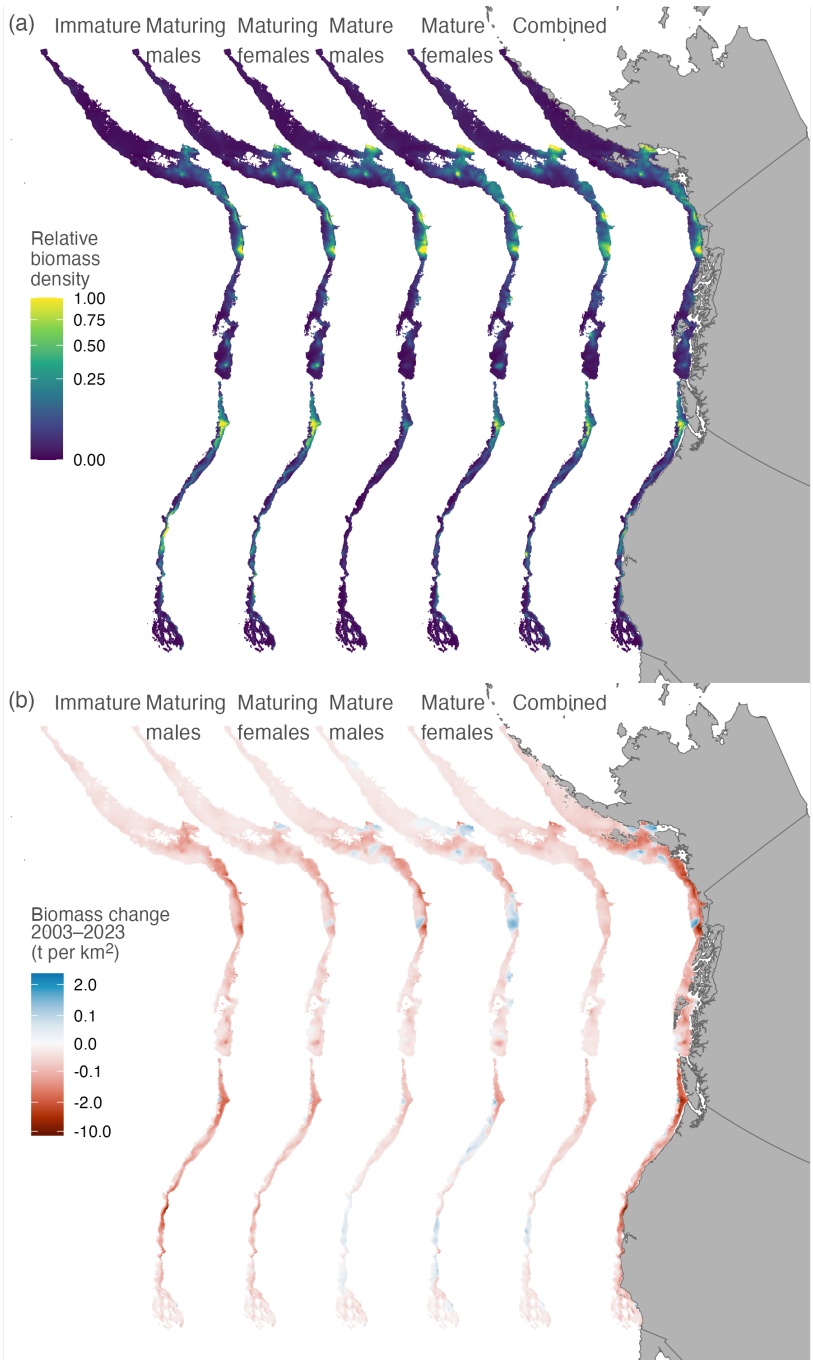

Figure 4: Coastwide distribution and spatially varying relative biomass trends for Dogfish for the period 2003–2023. (a) Coastwide relative biomass density in 2003 from trawl surveys. Biomass density is scaled between 0 and 1 and the colour scale is square root transformed. (b) Spatially varying biomass trends from a spatially varying coefficient model. Legend represents the difference in estimated biomass between 2003–2023 such that negative values reflect declines per grid cell of tonnes per km^2.

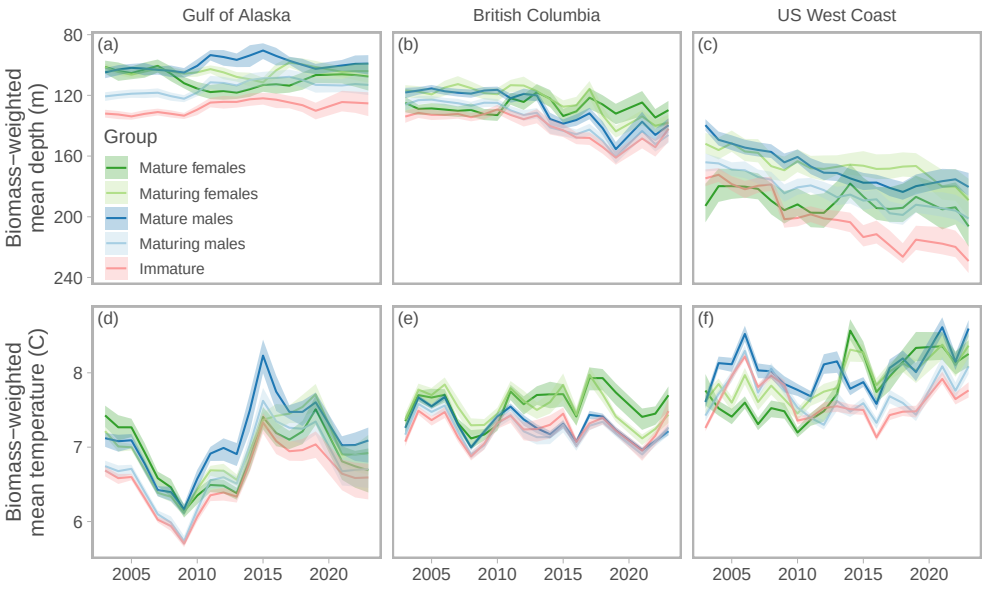

Figure 5: Biomass-weighted mean depth (a–c) and mean temperature (d–f) by region and maturity group. Lines represent the biomass-weighted mean depth or temperature and shaded ribbons represent 50% confidence intervals.

A Supporting Methods

A.1 Survey data

A.1.1 Trawl surveys

In total, we used data from ten bottom trawl surveys. These surveys consisted of four surveys conducted along the US West Coast (1980–2023), five within BC (1984–2023; Wyeth 2024), and one within the Gulf of Alaska (1993–2021; Figures S2, S4, S5, S6). These trawl surveys share similar random depth-stratified designs, fishing gear, and fishing protocols.

Trawl surveys along the US West Coast extend back to 1977 (Keller et al. 2017); however, the final US West Coast dataset we included consisted of four surveys: the annual West Coast Groundfish Bottom Trawl (WCGBT) surveys (2003–present), the AFSC triennial shelf "Triennial" survey (1980–2004), the annual NWFSC slope survey ("NWFSC.slope", 1998–2002), and the annual AFSC slope survey (with the exception on 1994 and 1998; "AFSC.slope", 1984–2001) (Keller et al. 2017, Wetzel et al. 2024) (Figure S1). The WCGBT trawl survey is completed twice annually since 2003: pass 1 is completed in the early spring and pass 2 is completed in the fall (Keller et al. 2017)(Figures S2, S1) . The spring and fall passes of the WCGBT survey are annual and have consistent timing and design since their implementation in 2003 (Keller et al. 2017, Wetzel et al. 2024) (Figures S1, S6, S6). Given the fact that Dogfish exhibit seasonal migrations along the coast, we chose to treat WCGBT spring and fall passes separately. Although the AFSC slope surveys began in 1984 from 1997 onwards is when the survey design, area surveyed, date of survey, became consistent. Similarly, the AFSC/NWFSC Triennial shelf surveys were completed between 1977–2004 but data from 1995 onwards is when the spatial and depth coverage and timing of the survey became consistent (Gertseva et al. 2021). We included the AFSC slope survey from 1997 until it ended in 2001 and Triennial survey from 1980 to 2004 but with a separate catchabilities from 1995 onward to account for changes in the latitudinal range, gear changes, survey timing, and depth coverage (Gertseva et al. 2021) (Figures S1, S6, S6). Therefore, we included seven surveys as a factor predictor for the US West Coast-specific model (grey in Figure 1g): WCGBT pass 1, WCGBT pass 2, NWFSC Slope survey, NWFSC Triennial early survey (1980–1992), NWFSC Triennial late survey (1995–2004), AFSC Slope survey early (1984–1996) and AFSC Slope late (1997–2001) (Figure S14). We select the spring pass of the WCGBT as the reference survey.

In BC, we include five surveys in the regional models. These surveys are mostly completed on a biennial basis and span the continental shelf and upper slope of most of BC's coast: West Coast Vancouver Island trawl survey (WCVI), West Coast Haida Gwaii survey (WCHG), Hecate Strait (HS) survey, Queen Charlotte Sound survey (QCS), and the Hecate Strait Multi-Species assemblage (HS MSA) (Figures S4, S3 Anderson et al. 2019, Wyeth 2024). Within each survey, the timing has been consistent across years but differs between surveys (Figures S6. Prior to 2003, the only consistently surveyed area along the BC coast was the HS MSA, which was mostly biennial from 1984 through 2003 but covered a limited portion of the coast (Wyeth et al. 2018).

The Gulf of Alaska (GOA) survey is completed as part of the Groundfish Assessment Program of the Alaska Fisheries Science Centre (AFSC) (NOAA Fisheries 2022) (Figures S5). This survey began in 1984; however, we use data from 1993 onward as the gear, tow duration, and boat specifications are standardized from this time (Tribuzio et al. 2022) . Note that 1993 survey was completed later in the year than subsequent surveys (Figure S6). This survey was triennial from 1993 and then biennial from 2001 (Figure S5) (NOAA Fisheries 2022).

Regional models included all the surveys described above in order to generate the longest time series possible. For the coastwide models, the surveys that provided relatively consistent spatial coverage in all regions started in 2003. We therefore combined all surveys from 2003 onwards in all our coastwide trawl models: the Gulf of Alaska trawl survey, four BC trawl surveys (HS, WCVI, WCHG, and QCS), and the US West Coast trawl survey (WCGBT spring and fall pass) Figure(S7).

A.1.2 Longline surveys

We included a coastwide longline survey that is completed annually by the International Pacific Halibut Commission ("longline") (IPHC; IPHC 2024). Although designed to sample Pacific Halibut (*Hippoglossus stenolepis*), indexing the relative abundance of Dogfish from this survey is possible as they are consistently encountered (Figure S8). Dogfish have been enumerated since 1998; therefore, the time series we used extends from 1998–2022 (IPHC 2024) (Figure S8). Importantly, Dogfish are enumerated on 20 hooks in some years and on all hooks in other years, which is accounted for in our models through an offset for hook count (Anderson et al. 2019, Edwards et al. 2023). The IPHC longline survey has a fixed station design with stations located at the intersections of an 18.52 km (10 nautical miles) square grid intended to span depths ranging from 18–732 m (IPHC 2024). At a randomly selected subset of these stations, eight skates of 100 (±5%) size 16/0 hooks with 18 ft (5.49 m) spacing between each hook were set between May 24th and September 15th with goal of keeping to the same month each time, however there is variability in survey times (IPHC 2022) Figure(S9).

We excluded IPHC survey points that were outside the standard sample design and those survey points that were part of a 2018 expansion set that sampled the inside waters of BC and Alaska. We also removed survey points from the inside waters of BC and US West Coast (Strait of Georgia and Puget Sound, respectively) to keep the footprint consistent with the other surveys. The inside Dogfish populations do have exchange with the outside populations. Previous work found that the BC inside populations had minimal exchange with the outside population (Mcfarlane and King 2002) while 14 of 17 tagged Dogfish from the inside Puget Sound population made distinct seasonal movements outside of Puget Sound each year and remained outside until the following summer (Andrews and Harvey 2013). For the US West Coast, the area sampled by the IPHC was much larger in 2017 so data and the prediction grid was limited to the core sampling area to avoid predicting on an area with only one year of data.

A.1.3 Splitting trawl survey data by maturity

We split surveyed catch weight by maturity and sex so that sex- and maturity-specific biomass density could be modeled through time and space. For these biomass indices split by maturity, we focus on the trawl survey data since the IPHC longline survey did not collect Dogfish lengths until 2011 and the trawl surveys catch a wider range of Dogfish lengths—the IPHC survey catches fewer small Dogfish (e.g., Figure S19).

First, we standardized length measurement types across surveys using previously determined calibration coefficients to represent total length extended (TL_{ext}; Tribuzio and Kruse 2012). These calibrations were 1.02 to convert total length with tail in the natural position, 1.20 to convert precaudal length, and 1.10 to convert fork length (Tribuzio and Kruse 2012). Second, we fit logistic maturity ogives to length-at-maturity data from DFO trawl survey data based on gonad and ovary development using DFO maturity classifications (Table S2).

Female Dogfish were classified as mature if they were ready to spawn (large ova, uterus lengthened) and males if claspers extended beyond the anal fin and were stiff. The male classifications align with those used in other regions; however, here we define females as mature if they are ready to spawn whereas other regions define maturity if individuals were pregnant or between pregnancies (Tribuzio et al. 2009). Not considered here is the possibility of shifts in length and maturity relationships through time (Taylor 2008) and the non-significant, but biologically meaningful difference in the length/maturity relationship in Alaska compared to BC (Tribuzio et al. 2009). We fit GLMMs (generalized linear mixed effects models) with mature vs. immature as the response, total length as the predictor, Bernoulli error, logit links, and random intercepts for sampling ID (Figure 2a).

We then categorized sampled Dogfish from trawl surveys into length groups: "immature", "maturing", or "mature" if their probability of maturity was $\leq$ 5%, 5–95%, or $\geq$ 95%, respectively (Figure 2). Immature, maturing, and mature males were categorized as those with $TL_{ext} \leq$ 65.1 cm, be-

tween 65.1–76.7 cm, or ≥ 76.7 cm, respectively. Females are larger than males and were categorized into the respective maturity groups if TL_{ext} was ≤ 77.0 cm, between 77.0–95.6 cm, or ≥=95.6 cm.

We used these sampled fish and their maturity assignments to partition the overall Dogfish catch weight for each survey set. We did not have weight for individual Dogfish samples in Gulf of Alaska, so we converted these counts to weight using a length-weight relationship fit to BC data. We similarly used this relationship to fill in any missing weights in the BC data. We then applied the proportion of sampled weight from each maturity class per sex to the total tow catch weight. Partitioning the catch by maturity class was not possible for 6% of trawl tows (2,158 tows of over 34,000 tows). No samples were collected on these tows and therefore there was no information with respect to the size and sex composition of these tows. The catch weight of the removed tows was small, ~ 10 kg.

A.1.4 Assigning depth to survey data

Although depth is typically collected with the trawl and longline sets, we needed to have a depth covariate that was consistently derived for both model fitting and prediction on a grid (for visualization and area-expansion as described below). Therefore, we assigned bottom depth to each survey and grid point using the marmap R package (Pante et al. 2023). Using the same data source for both fitting and prediction ensures there is no bias in the covariate between the model and prediction.

A.2 Model structure

A.2.1 Data likelihoods and linear predictor links

We required generalized linear model structures to model biomass density (trawl surveys) and count density (longline survey). Trawl survey biomass density, contains both zeros and positive continuous values, which can be a challenging form of data to fit. We applied a widely used delta ("hurdle") model formulation (Aitchison 1955) to model biomass density observations as a product of an encounter probability p and a positive catch rate given encounter r. Specifically, we used a Poisson-linked version of a delta model (Thorson 2018). This model describes two linear predictors (η_1, η_2) with one describing log group numbers density n and the other describing a weight per group w:

$$\log(n) = \eta_1,$$
$$\log(w) = \eta_2.$$

These get transformed (Thorson 2018) via

$$p = 1 - \exp(-\exp(\log n)),$$
$$r = \frac{nw}{p},$$

to model encounter probability (p) and positive catch rate (r). The first component is the inverse complementary log-log link; however, numbers (n) from the first linear predictor, also enter into the calculation of r. These encounter probabilities can then be entered into a Bernoulli likelihood and the positive catch rates into a likelihood for positive continuous data such as the gamma or log-normal. This formulation has several advantages over a "standard" delta model with linear predictors in logit and log link space (Thorson 2018) but primary advantages here are (1) a better fit to the data with the same number of parameters (higher log likelihood) and (2) given the shared link across the linear predictors, we can combine coefficients (such as those representing spatially varying trends). Anderson et al. (2024b) further describe this delta model.

Dogfish, which can have extreme catch events, presents challenges for modelling as observations can have heavier tails than expected by standard distributions such as the gamma or log-normal. For example, a single tow from the 2019 US West Coast fall survey captured an amount that is ~ 1,400 times larger than the mean and is twice the weight of the second highest catch in

the history of the survey (30,8301 kg and 16,585 kg, respectively) (Gertseva et al. 2021). Therefore, we considered, and selected, a model that allowed for a given probability of a given positive catch rate being drawn from a second distribution with the same dispersion but a higher mean. Specifically, the mixture distribution allowed for some probability, p, that a given observation, r, came from a second distribution with the same scale (ϕ) but a higher mean (μ_2 vs. μ_1) and is a simplified version of the approach described in Thorson et al. (2011). The observation likelihood for positive observations (using the log-normal as an example) is constructed as

$$r \sim (1 - p_m) \cdot \text{Lognormal}\left(\log \mu_1 - \frac{\phi^2}{2}, \phi\right) + p_m \cdot \text{Lognormal}\left(\log \mu_2 - \frac{\phi^2}{2}, \phi\right). \quad (1)$$

The expected value of observations y is then defined as $\mathbb{E}[y] = (1-p_m)\cdot\mu_1 + p_m \cdot \mu_2$ and the variance is defined as $\text{Var}[\log y] = (1-p_m)^2 \cdot \phi^2 + p_m^2 \cdot \phi^2$. The parameter μ_2 is constrained to always be larger than μ_1. During initial model exploration, we attempted to estimate the proportion parameter p_m, but had challenges with model convergence in some cases. Therefore, we chose to fix p_m to a value of 1% (i.e., allowing a 1% probability of an extreme event) based on exploration of quantile-quantile plots of residuals.

We evaluated a variety of potential likelihoods and link structures for the observations. For the catch weights from trawl surveys, these included: Bernoulli-gamma and Bernoulli-log-normal in both "standard" delta and Poisson-link delta configurations and then the standard and mixture versions of the Bernoulli-log-normal. For the coastwide model fit to all trawl catch data, the Poisson-link Bernoulli-log-normal model with a mixture on the log-normal had the lowest AIC and the best residual diagnostics (Figure S10). In some models fit to particular maturity groups or with spatially varying coefficients, we were forced to choose a simpler observation likelihood (Table S1). For the IPHC longline survey, which records counts of Dogfish, we considered a negative binomial likelihood where the variance scales linearly or quadratically with the mean (NB1 and NB2; Hilbe 2011), the Poisson likelihood, as well as a log-normal-Poisson likelihood where an observation-level random intercept is added to a Poisson model to account for additional dispersion. The NB2 had the lowest AIC and the best residual diagnostics (Figure S11).

A.2.2 Standard spatiotemporal model structure

Our spatiotemporal models followed a similar structure throughout with quadratic fixed effects for log bottom depth, spatial Gaussian Markov random field (GMRF) representing constant latent spatial processes, and a spatiotemporal GMRF following a random walk to account for latent spatiotemporal processes as well as all time variation in mean density.

Here we describe the spatiotemporal structure for a single linear predictor for simplicity. In practice, delta models used two linear predictors (described above) and count models (NB2) or Tweedie error models (Tweedie 1984) used a single linear predictor. Table S1 summarizes all model configurations.

We modelled the expected value $\mu_{\boldsymbol{s},t}$ at spatial coordinates $\boldsymbol{s}$ and time t as

$$\mu_{\boldsymbol{s},t} = g^{-1}\left(\beta_0 + \beta_1 D + \beta_2 D^2 + \omega_{\boldsymbol{s}} + \epsilon_{\boldsymbol{s},t}\right), \quad (2)$$

where g^{-1} represents an inverse link, β_0 represents an intercept (starting mean), D and D^2 represent orthogonal polynomials of log depth, β_1 and β_2 represent estimated effects of D and D^2, $\omega_{\boldsymbol{s}}$ represents a spatial GMRF effect, and $\epsilon_{\boldsymbol{s},t}$ represents a spatiotemporal random walk GMRF effect.

The $\omega_{\boldsymbol{s}}$ effects are assumed to follow a multivariate normal distribution with inverse precision (i.e., covariance) matrix Σ_ω

$$\boldsymbol{\omega} \sim \text{MVNormal}\left(\mathbf{0}, \Sigma_\omega\right), \quad (3)$$

where $\boldsymbol{\omega}$ represents a vector of $\omega_{\boldsymbol{s}}$ values. The $\epsilon_{\boldsymbol{s},t}$ effects are assumed to follow a random-walk GMRF process built by a series of $\boldsymbol{\delta}_t$ that are themselves drawn from a multivariate normal distri-

bution with inverse precision matrix Σ_ϵ

$$\boldsymbol{\delta}_t \sim \text{MVNormal}\left(\mathbf{0}, \Sigma_\epsilon\right), \tag{4}$$

$$\boldsymbol{\epsilon}_{t=1} = \boldsymbol{\delta}_{t=1}, \tag{5}$$

$$\boldsymbol{\epsilon}_{t>1} = \boldsymbol{\epsilon}_{t-1} + \boldsymbol{\delta}_t. \tag{6}$$

Both of these covariance matrices are constrained by a Matérn correlation function, each with their own estimated marginal standard deviations (σ_ω, σ_ϵ) and ranges (ρ_ω, ρ_ϵ). The range parameters represent the distance at which correlation has decayed to approximately 0.13, or more generally the distance at which two points are approximately independent (Lindgren et al. 2011).

This random walk random field can predict over missing years and spatial locations given the assumed correlation structure. This is especially useful when combining biennial or triennial surveys where spatial coverage alternates (Anderson and English 2022), or modelling surveys with inconsistent spatial coverage over time (DFO 2024). This model parameterization is similar to that used by the IPHC, who use a first-order autoregressive GMRF (Webster et al. 2020). Experimentation with letting mean density be estimated independently for each year or follow a process such as a random walk resulted in the mean process jumping around based on which surveys were present in a given year as the model confused spatial differences for temporal differences.

Our base models combined survey data across the Gulf of Alaska, BC, and the US West Coast. We checked that our combined model resulted in similar trends to region-specific models by applying the same model structure to regional data (Figure 1). In our coastwide model we restricted model fitting to data that started in 2003 when surveys were conducted in all regions. We considered models that estimated catchability effects relative to a base survey level by including survey name as a factor predictor (Figure S13). These models had larger standard errors, a similar overall trend, and were not favoured by AIC compared to a model without catchability effects (Figure S12).

A.2.3 Spatiotemporal models fit to survey data split by maturity

We fit similar models to the coastwide survey catch data split by maturity group. However, because the data were sparser, we encountered convergence issues with several maturity groups when fitting the mixture model described above. We therefore simplified all maturity-specific models to remove the mixture component (Table S1).

A.2.4 Spatially varying trend models

To assess hotspots of change in Dogfish density, we fit coastwide geostatistical models with spatially varying coefficients (Hastie and Tibshirani 1993) for time (decade) constrained as a GMRF (Barnett et al. 2021). We only fit these models to the trawl survey data (not the IPHC), since the trend from 2003 onwards could be reasonably approximated as an exponential change (linear in log link space) (Figure 1). We fit these models to the total set catch weight as well as to the catch weight split by maturity category. Due to convergence issues with some models, we (1) dropped the mixture component described above, (2) omitted spatiotemporal random effects and (2) employed a sequential set of families, fitting one and then moving to subsequent families if convergence issues were detected. These were a Poisson-link delta-lognormal family, a Poisson-link delta-gamma family, and finally a Tweedie observation model with a log link (Table S1).

Our spatially varying coefficient term was defined as decade centered on 2010 to improve interpretability and reduce correlation with the intercept. Since all fitted families employed log links, we could extract spatially varying trends per decade by summing the fixed and random decade coefficient effects. In the case of the Poisson-link delta models this entailed summing these components from the first and second linear predictor in link space. In the case of the Tweedie model, the single linear predictor represented the overall effect.

A.3 Model fitting

A.3.1 Software and parameter estimation

We fit all spatiotemporal models with the R (R Core Team 2024) package sdmTMB (Anderson et al. 2024b) version 0.6.0, which fits geostatistical linear mixed-effects models (GLMMs) using the Stochastic Partial Differential Equation (SPDE) approximation to Gaussian random fields (Lindgren et al. 2011) using Template Model Builder (TMB) (Kristensen et al. 2016). The sdmTMB package uses the fmesher package (Lindgren 2023) to generate input matrices to carry out the SPDE-based precision matrix calculations described in Lindgren et al. (2011). The marginal log likelihood and its gradient are calculated using TMB and the marginal negative log likelihood is minimized via the `nlminb()` non-linear minimization routine in R (R Core Team 2024) with a final Newton optimizer minimization step (accomplished via R's `optimHess()`) to further reduced the log likelihood gradient. Random effects are integrated over with the Laplace approximation and standard errors are calculated with the generalized delta method using TMB (Kristensen et al. 2016). A generic bias-correction algorithm is applied to account for bias due to non-linear transformations of random effects (Thorson and Kristensen 2016). We conducted all analyses in R version 4.4.0 (R Core Team 2024).

The implementation of the SPDE approach requires Delaunay triangulation meshes. These meshes are used both as part of the SPDE approach to precision matrix calculation (Lindgren et al. 2011) and for bilinear interpolation from the random effects (vertices in the mesh) to the data observation locations or prediction locations. We chose mesh designs to balance computational precision with speed and a triangulation was done with the `fmesher::fm_mesh_2d_inla()` function (Lindgren 2023) package version 0.1.5. Example meshes for the coastwide models used in Figure 1 are shown in Figures S17 and S18. We first defined an inner mesh using non-convex hulls drawn around the data observations with the `fmesher::fm_nonconvex_hull_inla()` function. For most coastwide and regional trawl models, mesh triangulation was constrained to have minimum and maximum triangle edge lengths of 30 and 45 km respectively within the inner area, maximum triangle lengths of 1000 km in outer area, and offsets from the data of 10 km and 300 km for each of these areas, respectively. For the main IPHC longline model and maturity-specific trawl models where data resolution was coarser, we used the same values except that the inner minimum edge length was increased to 50 km and the maximum to 55 km. Due to a much smaller total area, inner area minimum and maximum triangle edge lengths were reduced to 16 and 24 km respectively for the British Columbia trawl model. We aid estimation of random field standard deviation and range parameters and penalize them away from complexity (large magnitude wiggly fields) using bivariate penalized complexity priors (Fuglstad et al. 2015) specified as $P(\sigma < 2 = 0.95)$ and $P(\rho > 3 \times$ the minimum distance between mesh vertices $= 0.95)$.

A.3.2 Model checking and diagnostics

We assessed model convergence by ensuring the absolute marginal log-likelihood gradient with respect to all fixed effects was < 0.001, the Hessian was positive definite, and no random field marginal standard deviations were on a boundary (defined as < 0.01). We compared model parsimony, where described, using the marginal Akaike Information Criterion (AIC) (Akaike 1973). We evaluated distributional assumptions of the models with simulation-based randomized quantile residuals (Dunn and Smyth 1996, Smith 1985) using the DHARMa R package (Hartig 2022) (Figures S10, S11). When simulating from our model to calculate these residuals we took a single sample of the random effects from their approximate posterior (multivariate normal) distribution instead of using the empirical Bayes estimates (random effect values that maximize the log likelihood conditional on the fixed effects held at their MLEs) so that the residuals would have the desired distributional properties if the model were consistent with the data (Waagepetersen 2006, Thygesen et al. 2017).

A.4 Calculating total biomass/abundance and density-weighted depth

To visualize spatial predictions, calculate area-weighted indices of abundance, and calculate biomass-weighted mean depth, we required a discretized grid covering the domain of the surveys.

A.4.1 Defining prediction grids

For the trawl surveys, we generated a convex hull over the previously generated survey domains from the regional grids (Keppel and Grandin 2022, Ward et al. 2023). A 25 km buffer was added to the convex hull to ensure there was continuity between jurisdictional borders. Within this new coastwide survey domain we then created a 4 km × 4 km grid (16 km^2) grid using an Albers projection using the 1/6 and 5/6 latitude quantiles from all trawl survey data (38.5 and 56.0 respectively). The centroid of each grid cell was assigned a depth using marmap (Pante et al. 2023) and truncated to depths greater than 15 m—the shallowest depth surveyed in all regions. We also calculated the area of each grid cell. Some cells were along the edge, or over land or islands, resulting in some cells having less than the full cell area.

The grid generation methods for the IPHC survey follow the methods to create the trawl prediction grid. We generated a convex hull around all surveyed IPHC stations, created a 25 km^2 buffer around the convex hulls, generated a 3 km × 3 km grid (9 km^2) grid in the Albers projection detailed above with depth assigned to the centroid of each grid cell using marmap (Pante et al. 2023). The US West Coast, however, is inconsistently sampled by the IPHC with the survey extending farther south in 2013, 2014, and 2017. The final prediction grid does not include these survey points that extend further south as predicting on these areas that are infrequently sampled creates an index with higher variability. Additionally, surveying in the US West Coast commenced a year later than other regions.

We assigned temperature values to the prediction grid to understand climate preferences through time and to calculate density-weighted mean temperature. To have a grid with complete coverage of temperature data, we generated predictions of gridded bottom temperature data using the temperature observations from each of the trawl surveys in our analysis (Wyeth 2024, Keller et al. 2017, Wetzel et al. 2024, NOAA Fisheries 2022). The bottom temperature measurements from each of the trawl surveys were modeled as the response variable with penalized regression splines on depth and julian date centred on July 1st, 2023. Spatial fields and spatiotemporal fields with an AR1 field were included to allow mean bottom temperature to be slightly different in each year and to vary in a non-linear pattern over time (methods e.g., Ward et al. 2024). Finally, we used a Tweedie distribution.

A.4.2 Area expansion for indexes of biomass/abundance

We expanded biomass and abundance density estimates at the cell level to total biomass or abundance by predicting on the survey domain grid, multiplying each density by cell area, and summing these values. This is a form of Monte Carlo integration (Thorson and Kristensen 2024). We calculated uncertainty on these summed values via the generalized delta method as implemented in TMB (Kristensen et al. 2016). We applied a generic bias correction method to account for the non-linear (exponential) transformation of the random effects in the cell-level predictions (Thorson and Kristensen 2016).

A.4.3 Biomass-weighted mean depth

We calculated biomass-weighted mean depth by predicting biomass density for each cell, multiplying the density by cell area to expand to biomass, and then taking the biomass-weighted mean depth across grid cells. We derived uncertainty on this value by simulating parameter values from the joint parameter precision matrix 200 times and taking the upper and lower quartiles of these samples.

B Supporting Tables

Table S1: Spatiotemporal model structures. All delta families are Poisson-link (Thorson 2018) delta models. The suffix "-mix" refers to a mixture model in which there is a 1% probability of an observation coming from a distribution with a higher mean. The two entries in the "Spatial" and "Spatiotemporal" columns refer to the two delta model linear predictors. "SVC" refers to spatially varying coefficients. "Mesh vertices" refers to the number of vertices in the SPDE mesh.

Model	Family	Spatial	Spatiotemporal	SVC	Mesh vertices
Coastwide trawl index	delta-lognormal-mix	on, on	rw, rw		1227
Coastwide longline index	NB2	on	rw		475
Regional trawl index (British Columbia)	delta-lognormal	off, off	rw, rw		461
Regional trawl index (Gulf of Alaska)	delta-lognormal	on, off	rw, rw		719
Regional trawl index (US West Coast)	delta-lognormal-mix	on, off	rw, rw		406
Coastwide trawl index (Immature)	delta-lognormal	on, on	rw, rw		537
Coastwide trawl index (Maturing females)	delta-lognormal	on, on	rw, rw		537
Coastwide trawl index (Maturing males)	delta-lognormal	on, on	rw, rw		537
Coastwide trawl index (Mature females)	delta-lognormal	on, on	rw, rw		537
Coastwide trawl index (Mature males)	delta-lognormal	on, on	rw, rw		537
Coastwide trawl SVC	delta-lognormal-mix	on, on	off, off	year	1226
Coastwide trawl SVC (Immature)	delta-lognormal	on, on	off, off	year	1226
Coastwide trawl SVC (Maturing females)	delta-gamma	on, on	off, off	year	1226
Coastwide trawl SVC (Maturing males)	delta-lognormal	on, on	off, off	year	1226
Coastwide trawl SVC (Mature females)	Tweedie	on	off	year	1226
Coastwide trawl SVC (Mature males)	delta-lognormal	on, on	off, off	year	1226

Maturity Codes for Pacific Spiny Dogfish (*Squalus acanthias*)

GFBIO MATURITY CONVENTION 10

Males			
Claspers	**Testes**	**Maturity Code**	**Maturity Stage**
Claspers do not extend past tips of anal fins.	Testes flat creamy.	10	Immature
Claspers extend past tips of anal fins; not stiff.	Testes, even creamy colour, not brown.	30	Maturing
Claspers extend past tips of anal fins; stiff.	Testes, creamy-brown, bloodshot, very firm.	90	Mature

Females			
Ovaries	**Uterus**	**Maturity Code**	**Maturity Stage**
Ova small, 0-5 mm diameter, white firm; ovary<1/4 length of body cavity.	Thin, no thickening.	10	Immature
Ova 5-10mm diameter, white, firm; ovary flaccid, flocculent external surface.	Thin, no thickening.	50	Immature
	Thin, <5mm thickened section; <1/4 length of body cavity.	51	Immature
	About 5mm thickened section; < 1/4 length of body cavity.	53	Immature
	Thickened section at least 10mm or wider, flaccid; >1/3 length of body cavity.	55	Maturing
	Encapsulated uterine eggs (candles).	56	Maturing
Ova <30mm diameter, yellow, firm.	Thin, no thickening.	70	Maturing
	Thin, <5mm thickened section; <1/4 length of body cavity.	71	Maturing
	About 5mm thickened section; < 1/4 length of body cavity.	73	Maturing
	Thickened section at least 10mm or wider, flaccid; >1/3 length of body cavity.	75	Maturing
	Yolk sac pups.	77	Mature
	Term pups (no yolk sac).	78	Mature
	Flaccid and empty.	79	Mature
Yellow ova firm and > 30 mm diameter along with white ova <10mm diameter; ovary flaccid, 1/3 length of body cavity.	Thickened section at least 10mm or wider, flaccid; >1/3 length of body cavity.	95	Mature
	Yolk sac pups.	97	Mature
	Term pups (no yolk sac).	98	Mature
	Flaccid and empty.	99	Mature

Table S2: Scheme used to categorized based on gonadal and ovary development of Dogfish sampled at sea in BC. These data were used to generate the maturity ogive which then informed our maturity categorizations Figure 2. To develop the ogive, male individuals with gonadal development stage 30 or higher and female individuals with ovary development stages 55 or higher, were categorized as mature.

C Supporting Figures

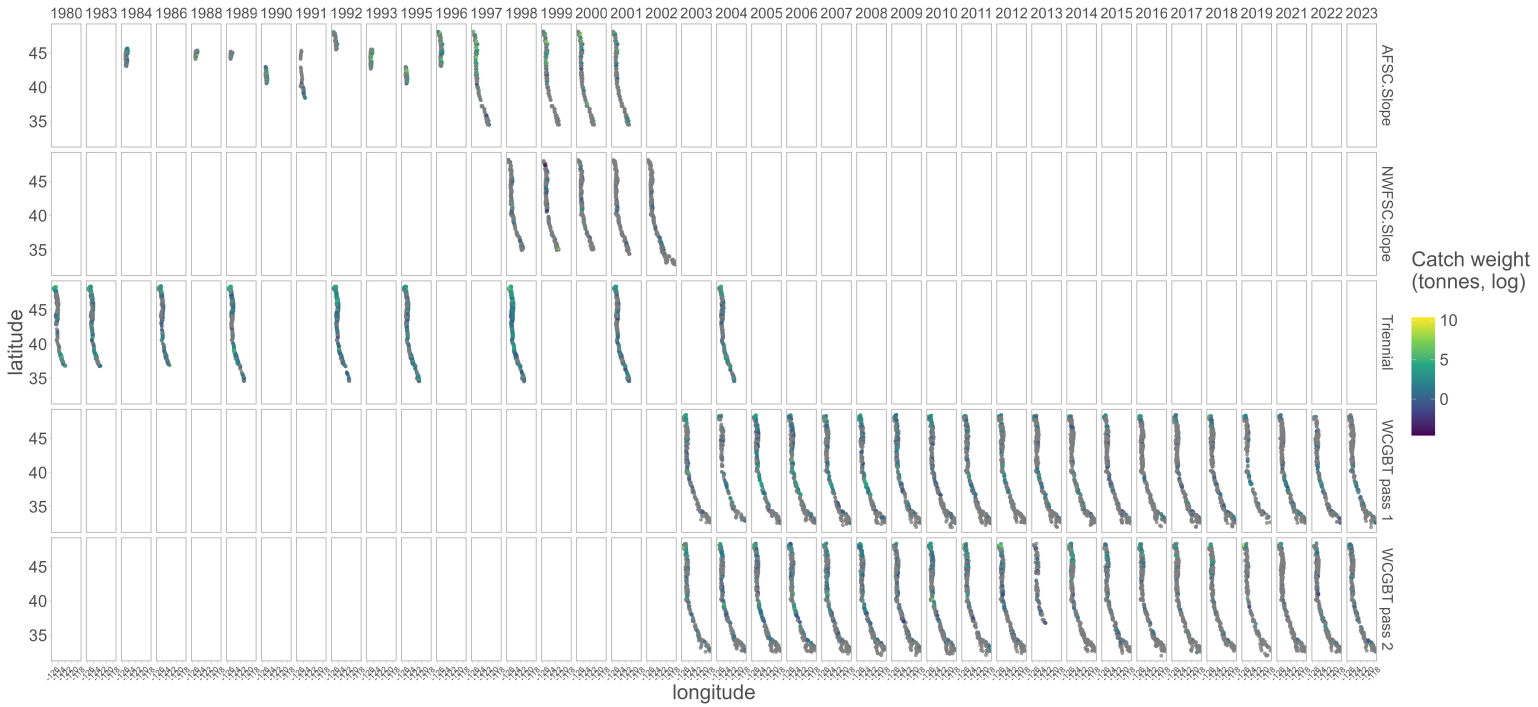

Figure S1: Distribution and catch weight of Dogfish in four trawl surveys on the US West Coast. In this analysis, survey catchability was estimated independently for seven groups: WCGBT pass 1, WCGBT pass 2, NWFSC Slope survey, NWFSC Triennial early survey (1980–1992), NWFSC Triennial late survey (1995–2004), AFSC Slope survey early (1984–1996), and AFSC Slope late (1997–2001).

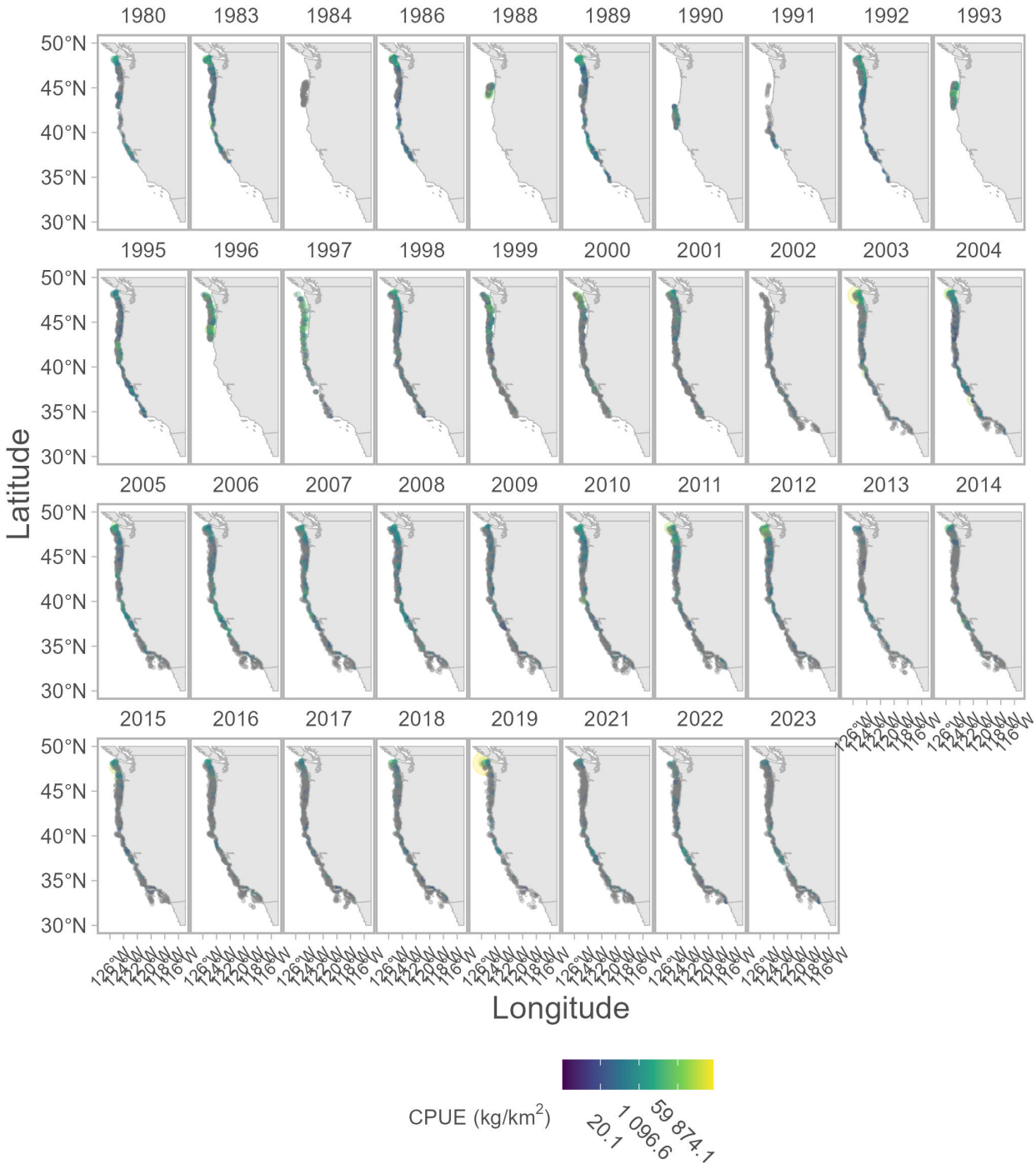

Figure S2: Distribution and catch weight of Dogfish in four trawl surveys on the US West Coast. These data generated the longest time series possible while the coastwide index included surveys from 2003 onwards.

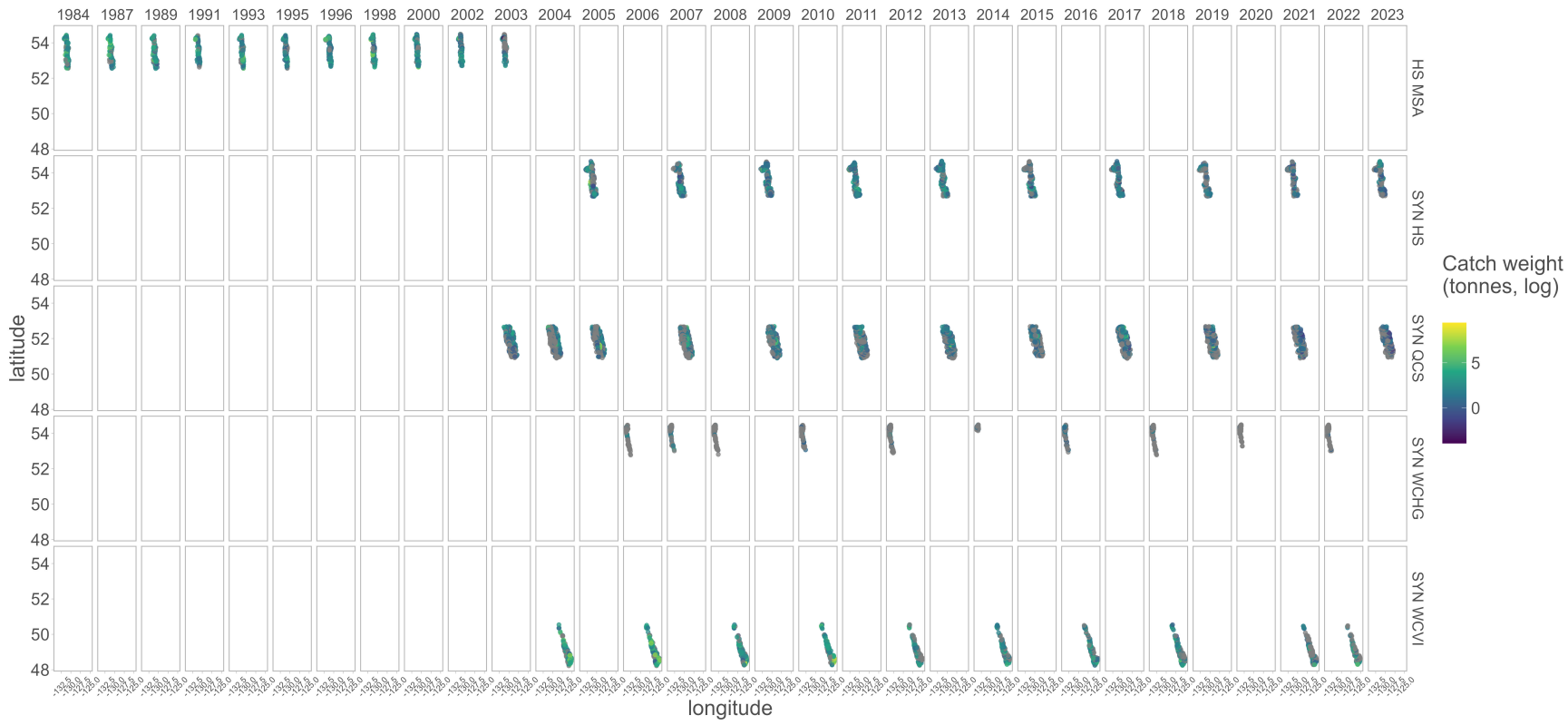

Figure S3: Distribution and catch weight of Dogfish in five trawl surveys in British Columbia, Canada. In this analysis, surveys were considered to have the same catachability as the gear—protocols are the same across the different surveys. Surveys include: HS MSA - Hecate Strait Multi-species assemblage, SYN HS - synoptic Hecate Strait, SYN QCS - synoptic Queen Charlotte Sound, SYN WCHG - synoptic West Coast Haida Gwaii, syn WCVI - synoptic West Coast Vancouver Island. These surveys were used to generate the longest time series possible for BC, however the more robust and coastwide analysis includes surveys from 2003 onwards.

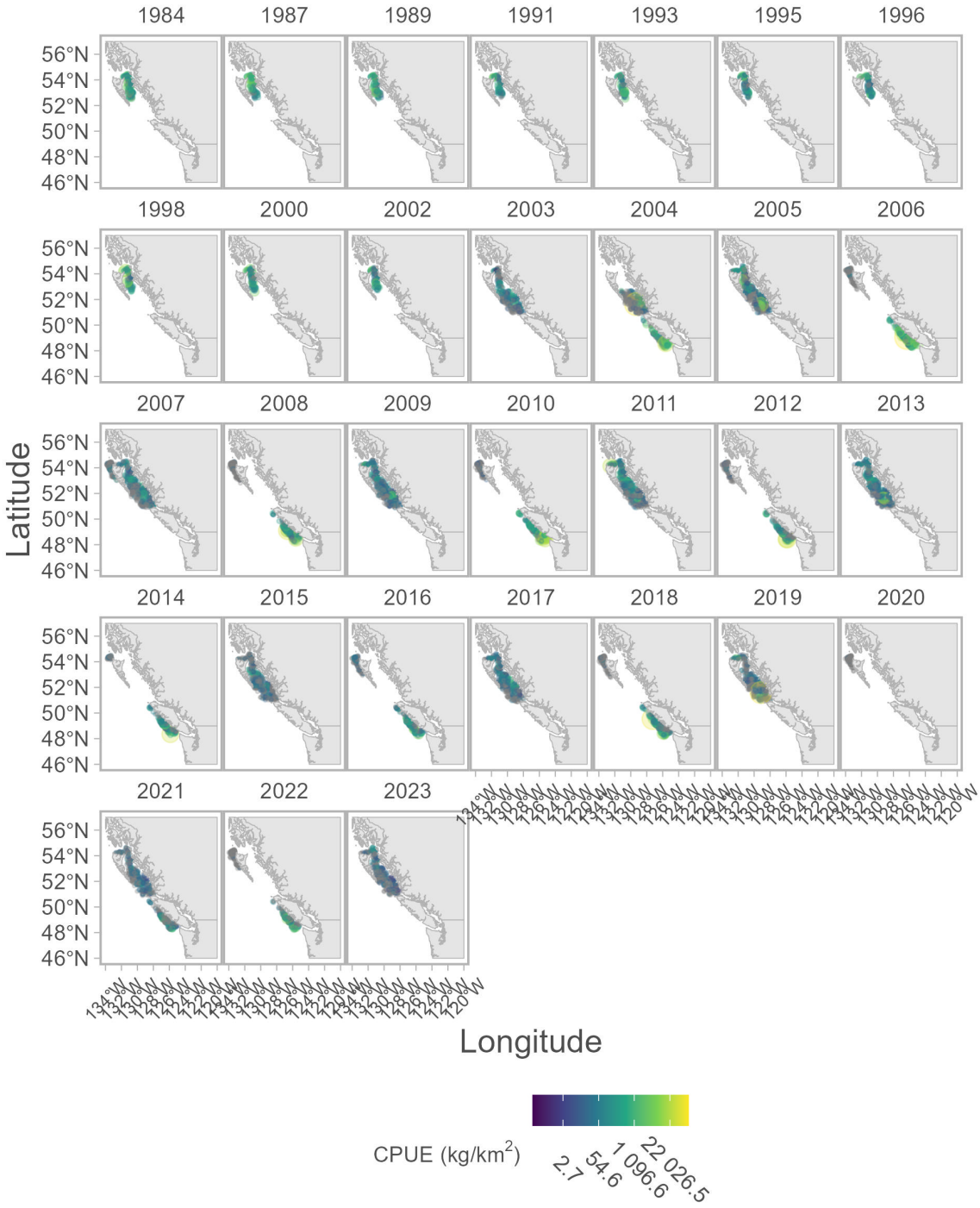

Figure S4: Distribution and catch weight of Dogfish in five synoptic bottom trawl surveys completed in British Columbia, Canada. Note the limited spatial distribution of the HS MSA completed between 1984–2002 that was used to make predictions across the coast.

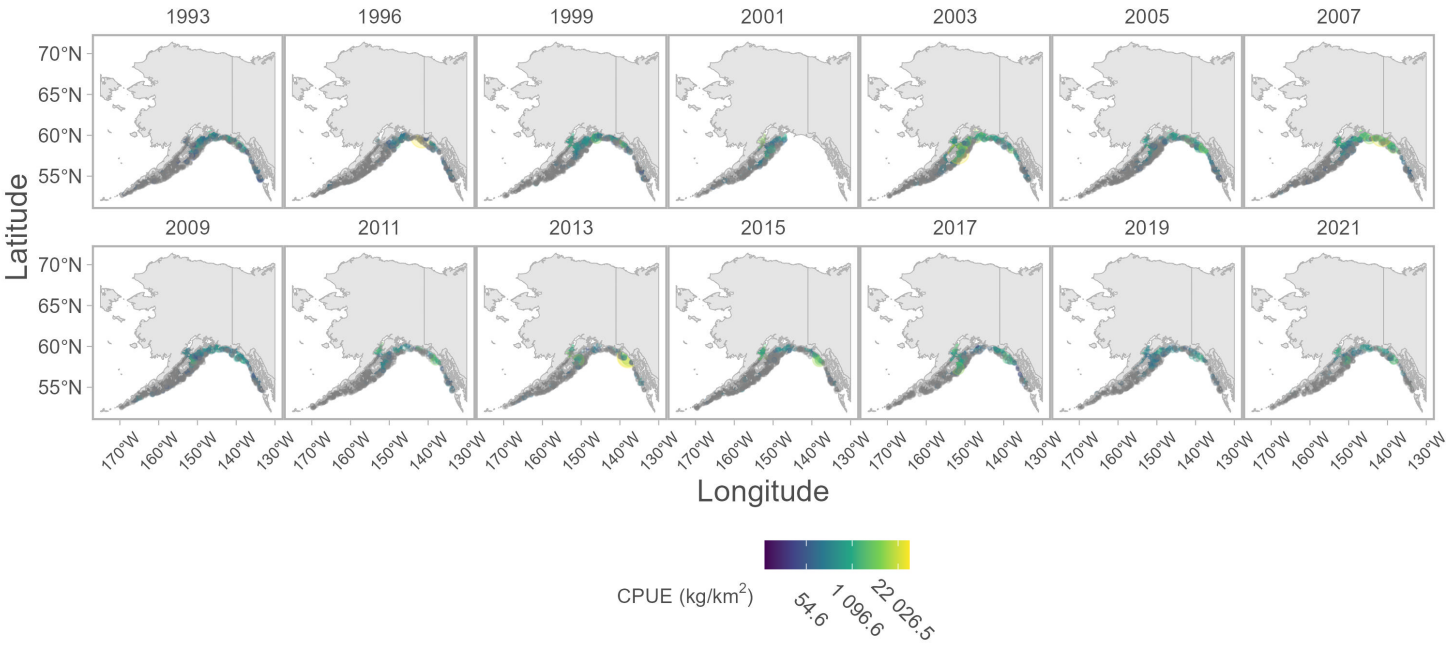

Figure S5: Distribution and catch weight of Dogfish in the Groundfish Assessment Program of the Alaska Fisheries Science Centre (AFSC) trawl survey. This survey began in 1984; however, we use data from 1993 onward as the gear, tow duration, and boat specifications are standardized from this time.

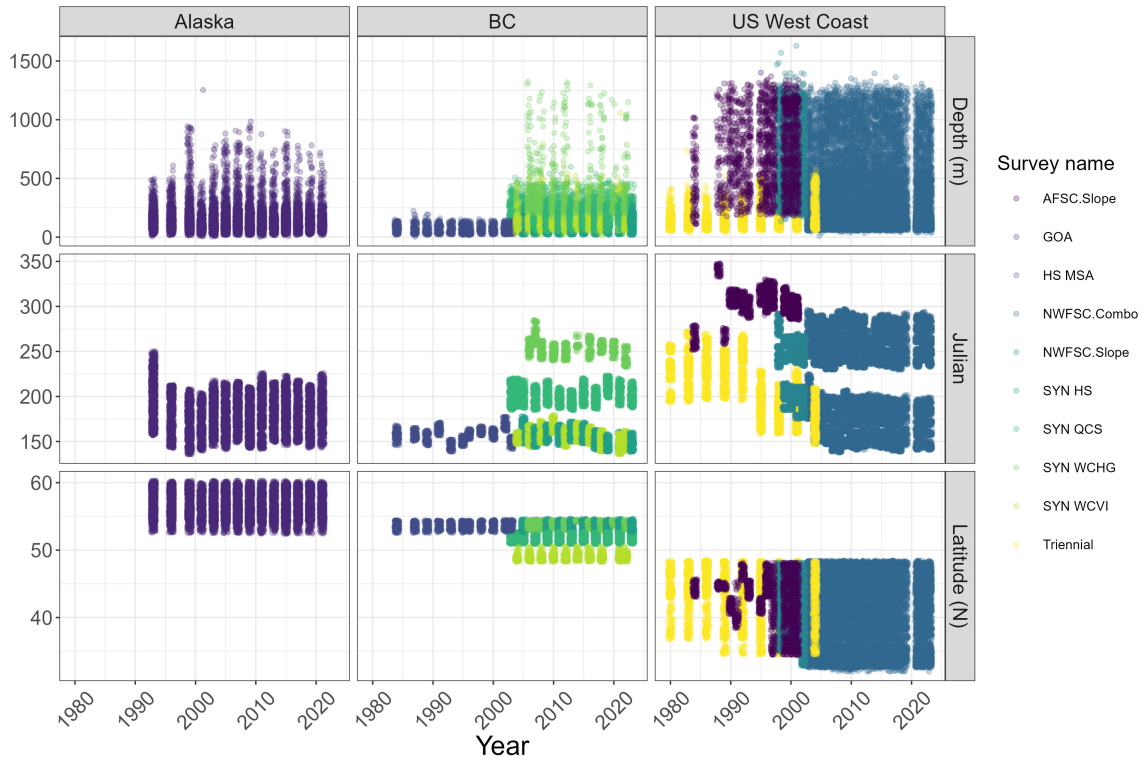

Figure S6: Variability in depth sampled, Julian date, and latitude for each of the trawl surveys included in the regional models.

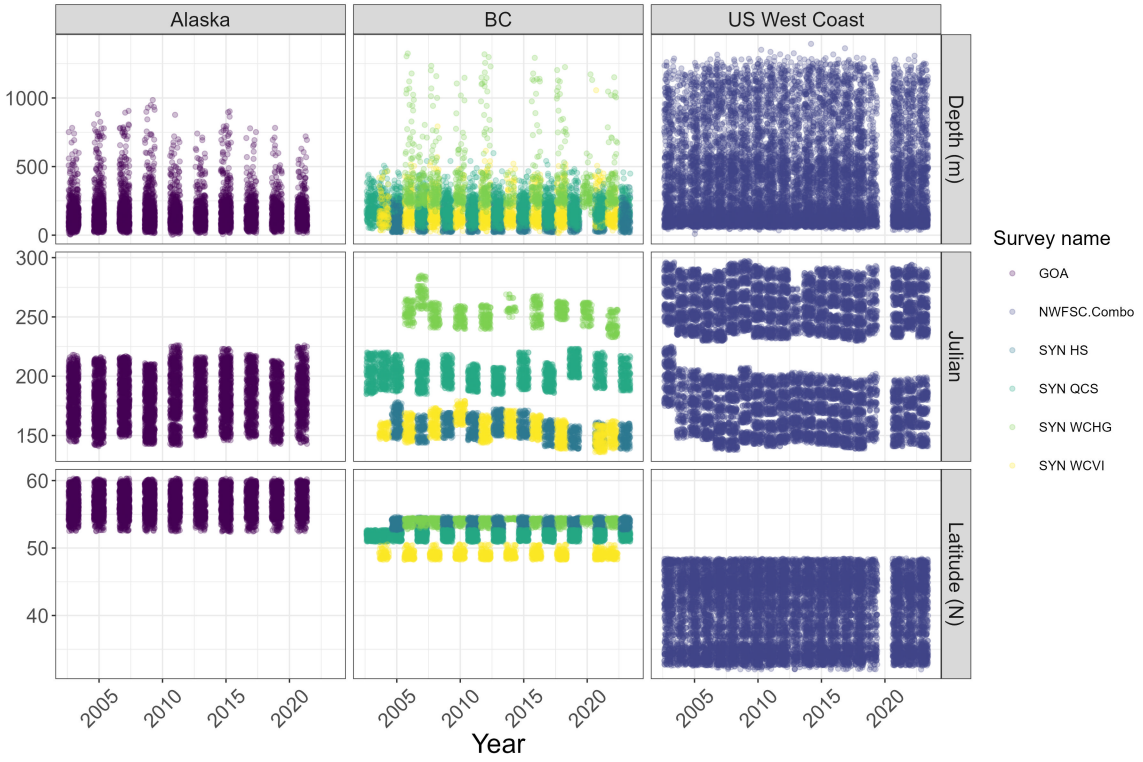

Figure S7: Variability in depth sampled, Julian date, and latitude for each of the trawl surveys included in the coastwide model from 2003 onwards. The year 2003 represents when there are consistent surveys available in all regions.

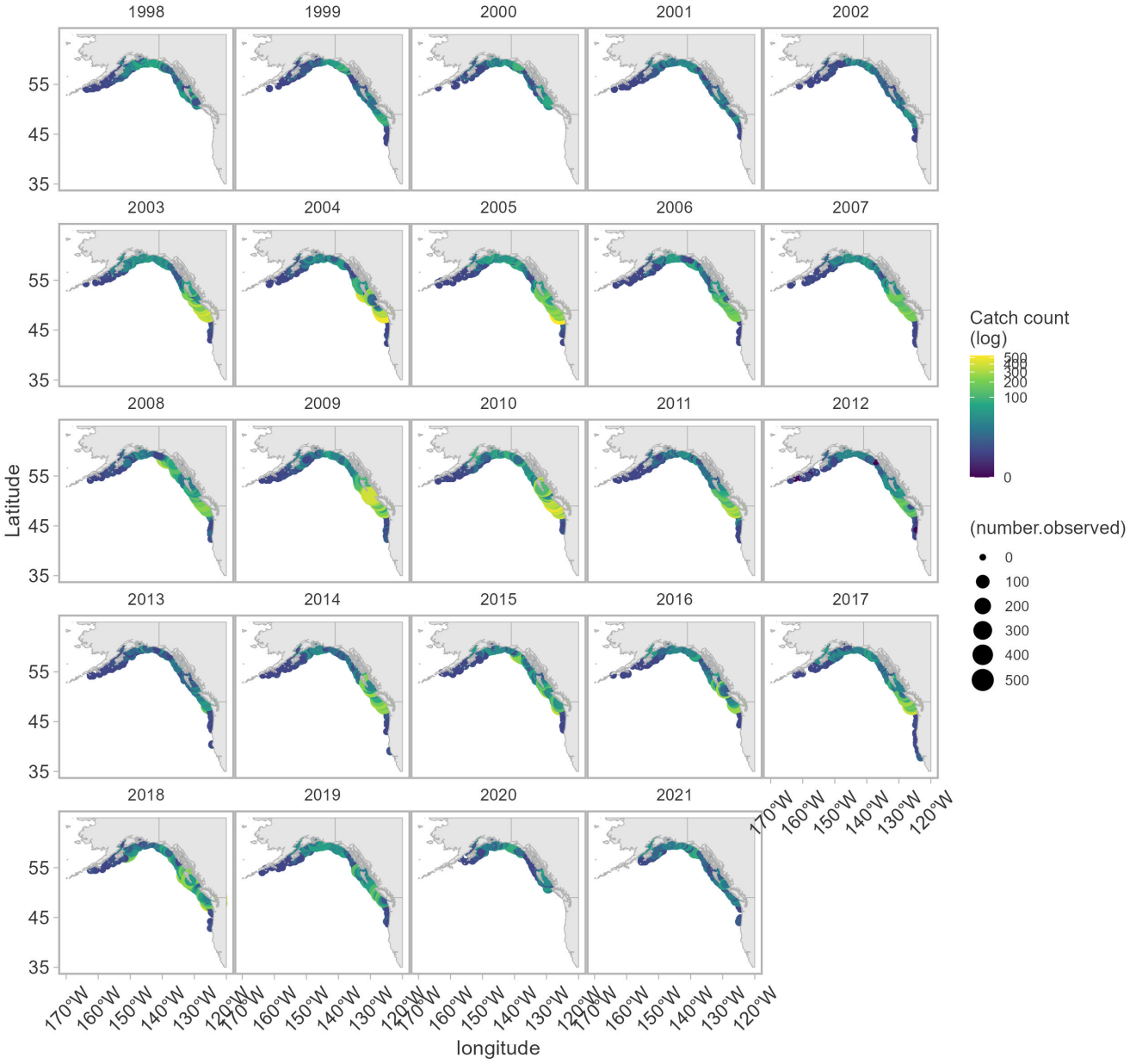

Figure S8: Distribution of catch counts of Dogfish for IPHC setline survey sets.

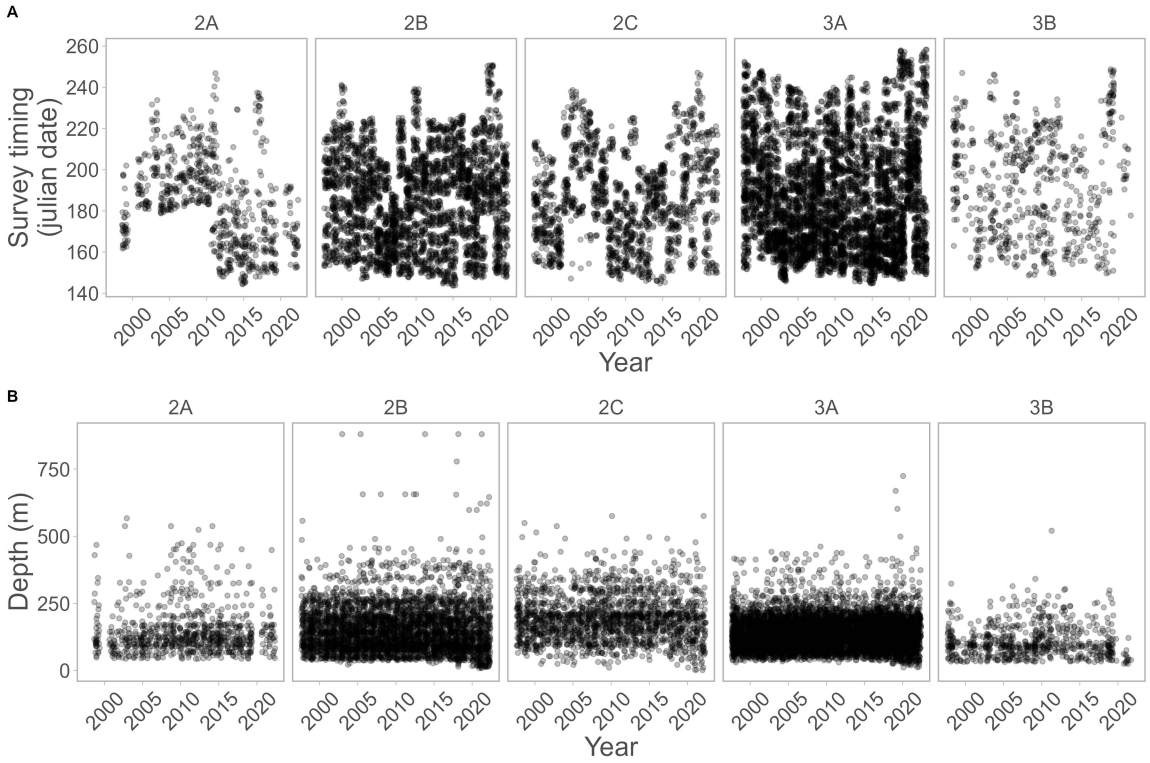

Figure S9: Variability in depth and survey timing for the IPHC survey in each region (US West Coast = 2A, British Columbia = 2B, Alaska = 2C, 3A, and 3B).

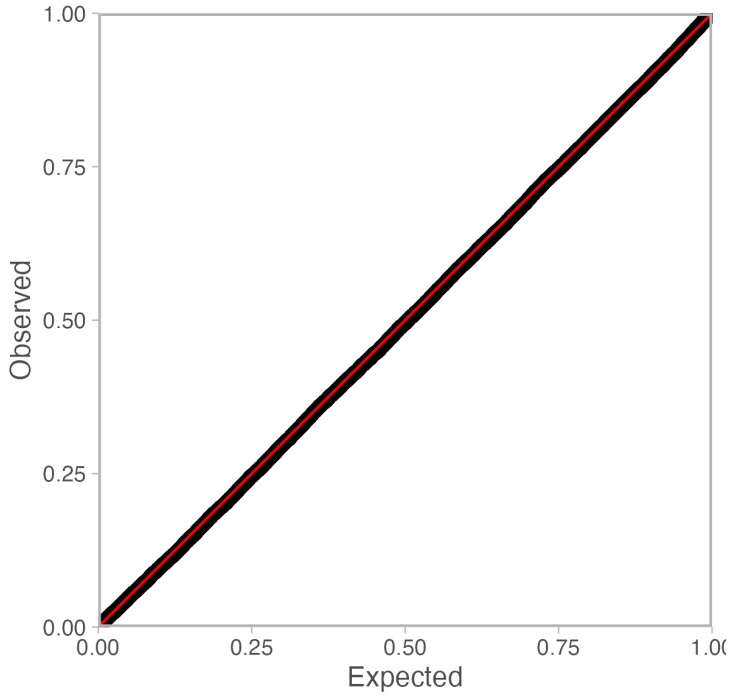

Figure S10: Quantile-quantile (QQ) plot for the coastwide trawl survey model with a Poisson-link delta-lognormal family where the lognormal includes a mixture of regular and "extreme" catch events. Dots represent randomized quantile residuals transformed to be uniformly distributed between 0 and 1 if the data are consistent with the distributional assumptions. Red line is a one-to-one line.

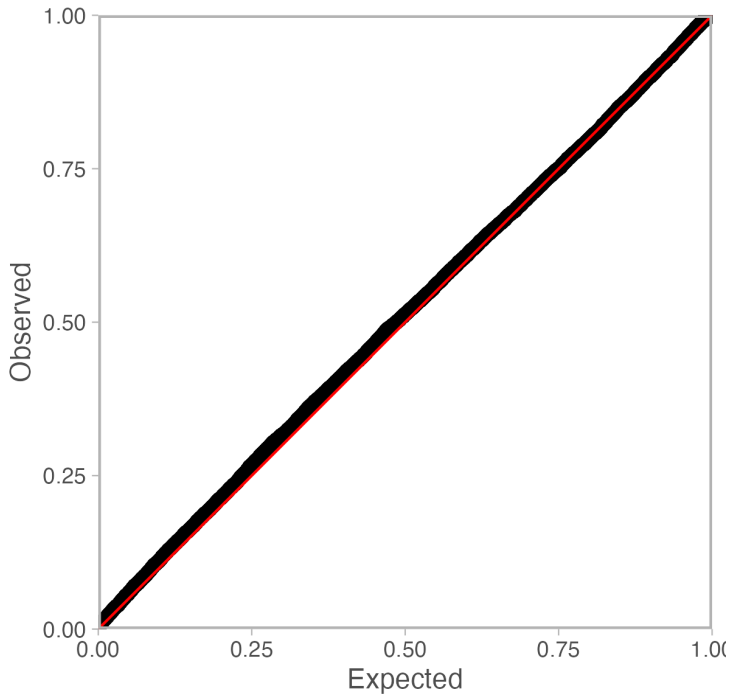

Figure S11: Quantile-quantile (QQ) plot for the coastwide IPHC setline model with a negative binomial observation error and log link. See Figure S10 for a full description.

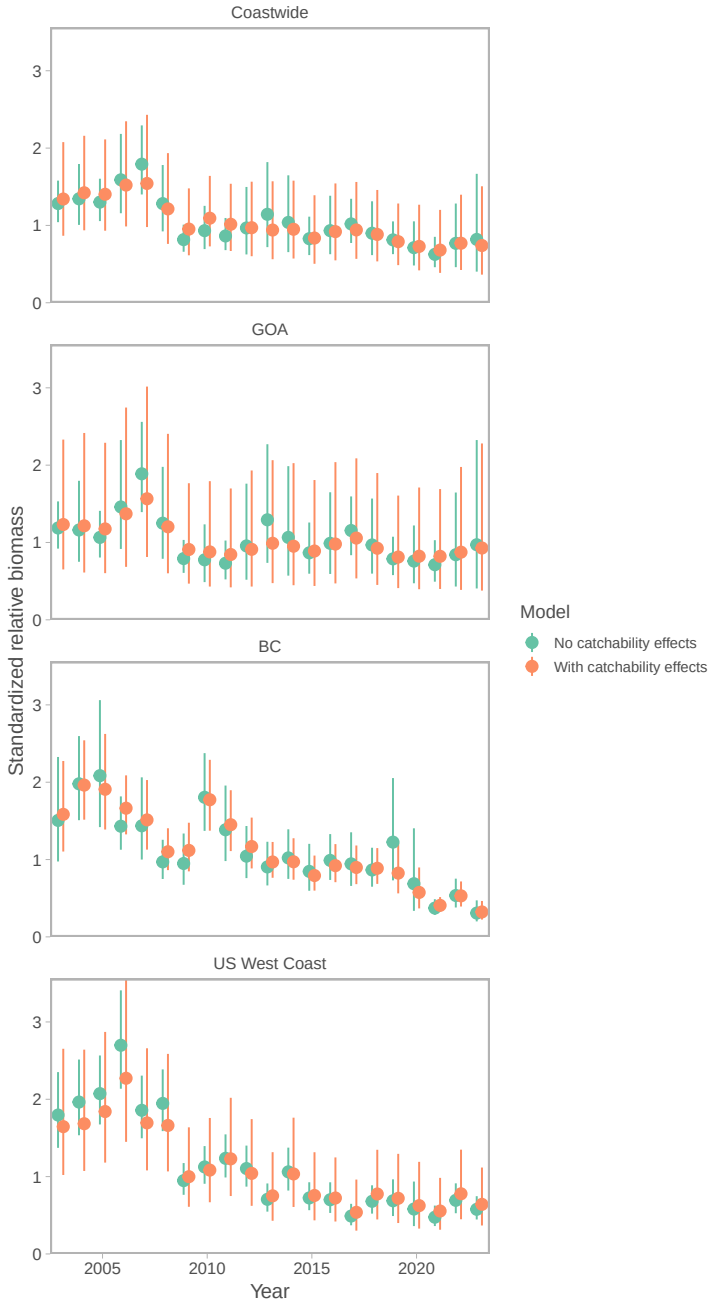

Figure S12: Coastwide trawl survey models with and without survey specific catchability effects estimated. Figure 1 presents the model without catchability effects estimated. Estimating catchability effects adds uncertainty to annual index estimates without changing the overall pattern. The model without catchability effects is favoured by AIC and survey gear and protocols are similar.

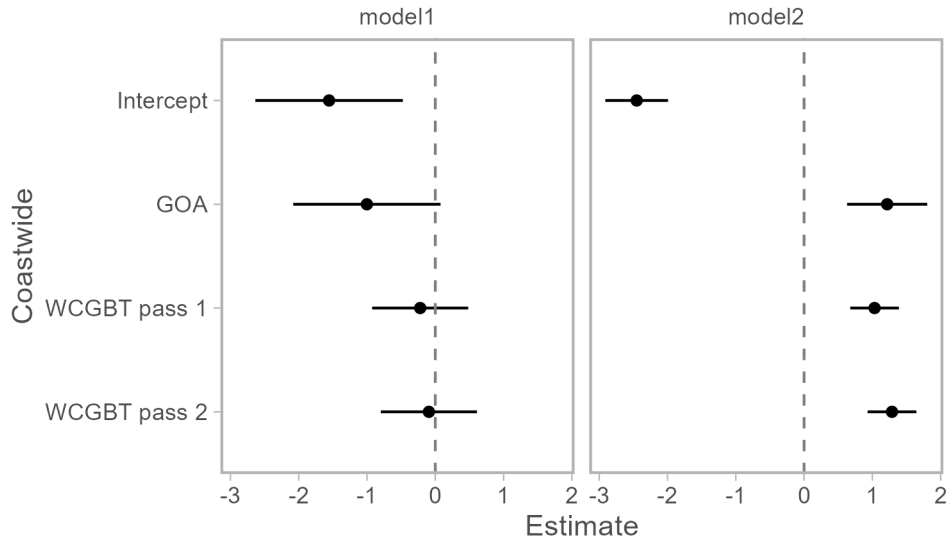

Figure S13: Estimated coefficients describing the catchability for the different surveys included in the model as factors for the coastwide analysis. Model 1 and 2 refer to the first and second linear predictors in the delta model. Estimates are shown in link space (log). The intercept is the BC level and the other levels represent deviations from the intercept.

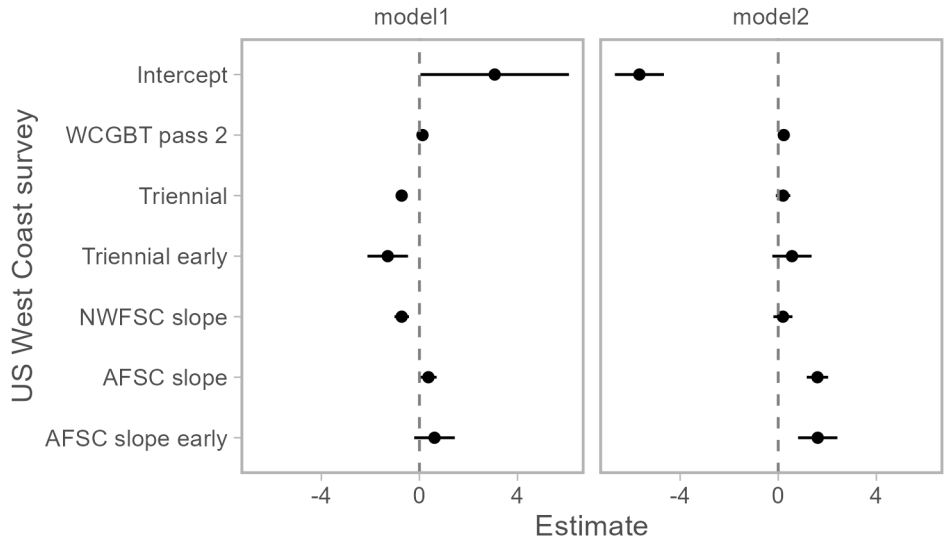

Figure S14: Estimated coefficients describing catchability for the different surveys included in the model as factors for the US West Coast-specific model. Model 1 and 2 refer to the first and second linear predictors in the delta model. Estimates are shown in link space (log). The intercept is the WCGBT pass 1 level and the other levels represent deviations from the intercept.

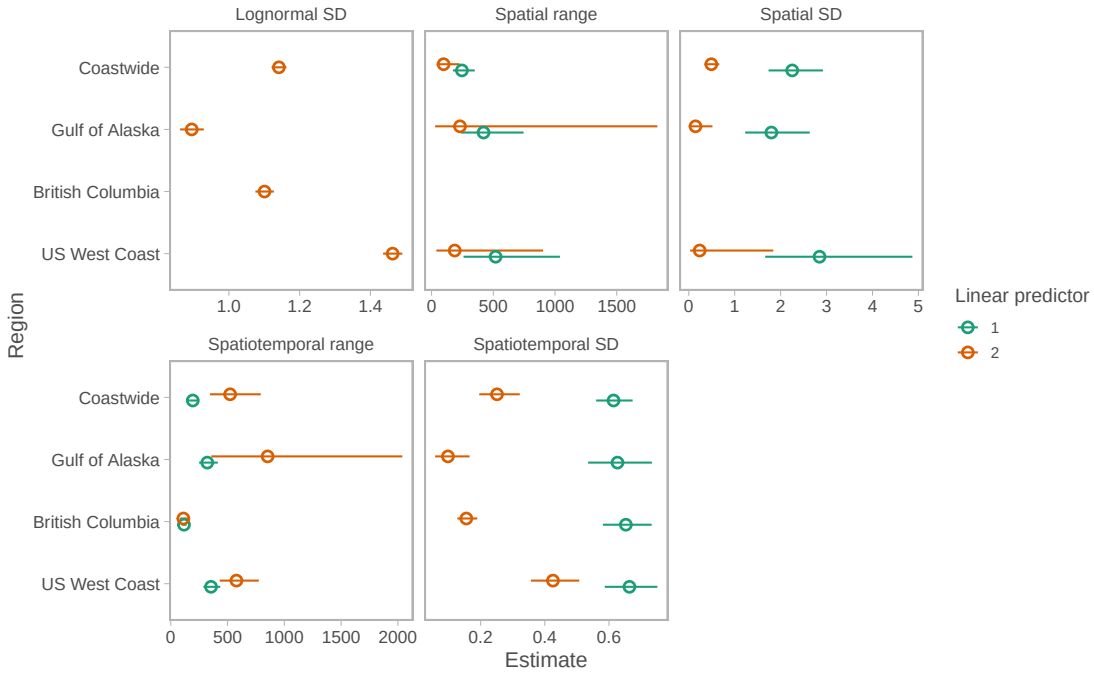

Figure S15: Observation error and Gaussian Markov random field Matérn correlation function parameter estimates for the coastwide and regional trawl survey models. Dots and lines indicate means and 95% confidence intervals.

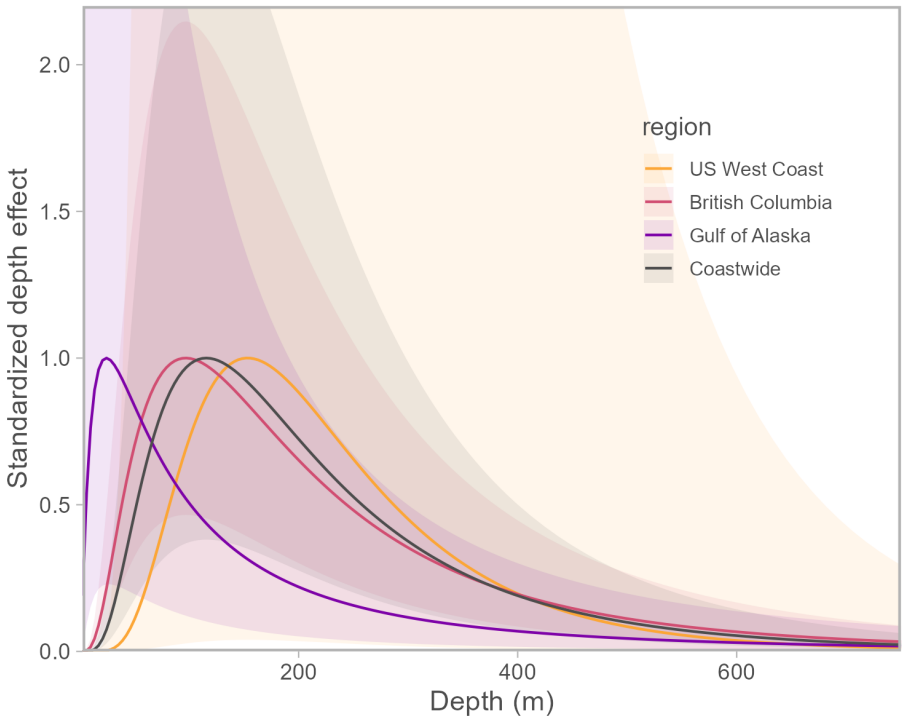

Figure S16: Quadratic depth effects estimated from the coastwide and regional spatiotemporal models fit to trawl survey data. Lines and ribbons indicate means and 95% confidence intervals.

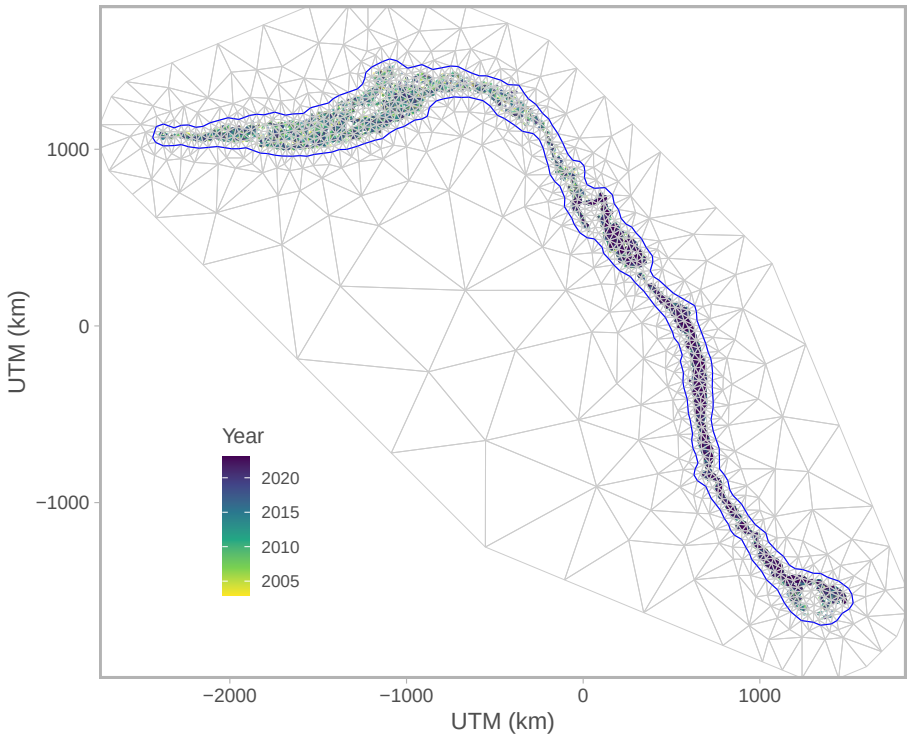

Figure S17: Delaunay triangulation mesh used in coastwide trawl survey modelling. Vertices are wherever triangle corners meet. This mesh is used as part of the SPDE precision matrix calculations (Lindgren et al. 2011) and in bilinear interpolation from the location of the random effects (at vertices) to the locations of the data observations or predictions. The blue line denotes a boundary where the triangles are coarser outside the boundary than inside (to balance computational precision and speed). Survey observations are shown as translucent dots coloured by year sampled.

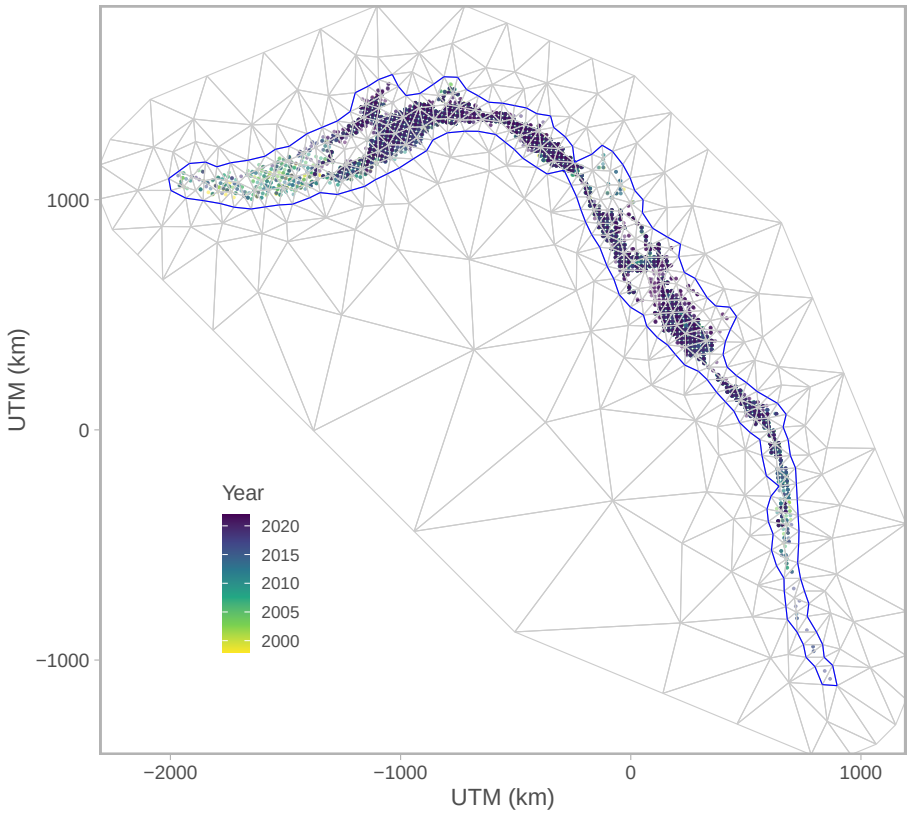

Figure S18: Delaunay triangulation mesh used in coastwide IPHC longline survey modelling. See Figure S17 for a complete caption.

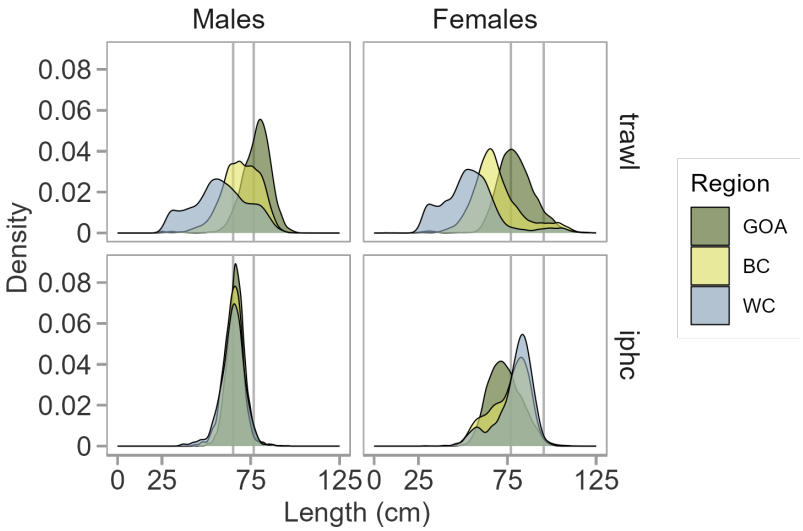

Figure S19: Density distribution of captured lengths across regions and geartypes.

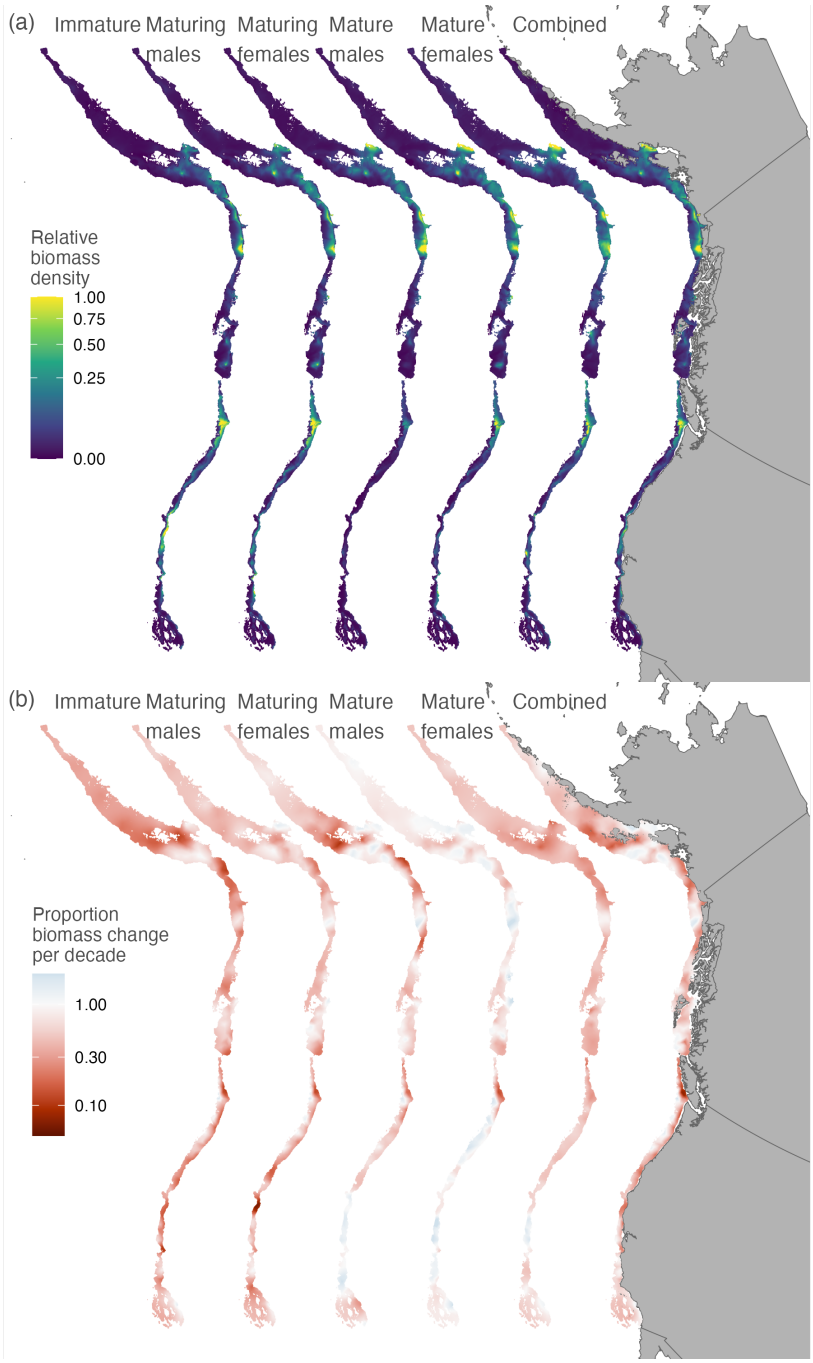

Figure S20: Coastwide distribution and spatially varying relative biomass trends for Dogfish for the period 2003–2022. (a) Coastwide relative biomass density in 2003 from trawl surveys. Biomass density is scaled between 0 and 1 and the colour scale is square root transformed. (B) Spatially varying biomass trends from a spatially varying coefficient model. A proportional change of 0.3, for example, represents a 70% decline per decade. Panel (a) is the same as Figure 4 but panel (b) here is plotted as proportional decline instead of absolute decline in biomass weight.

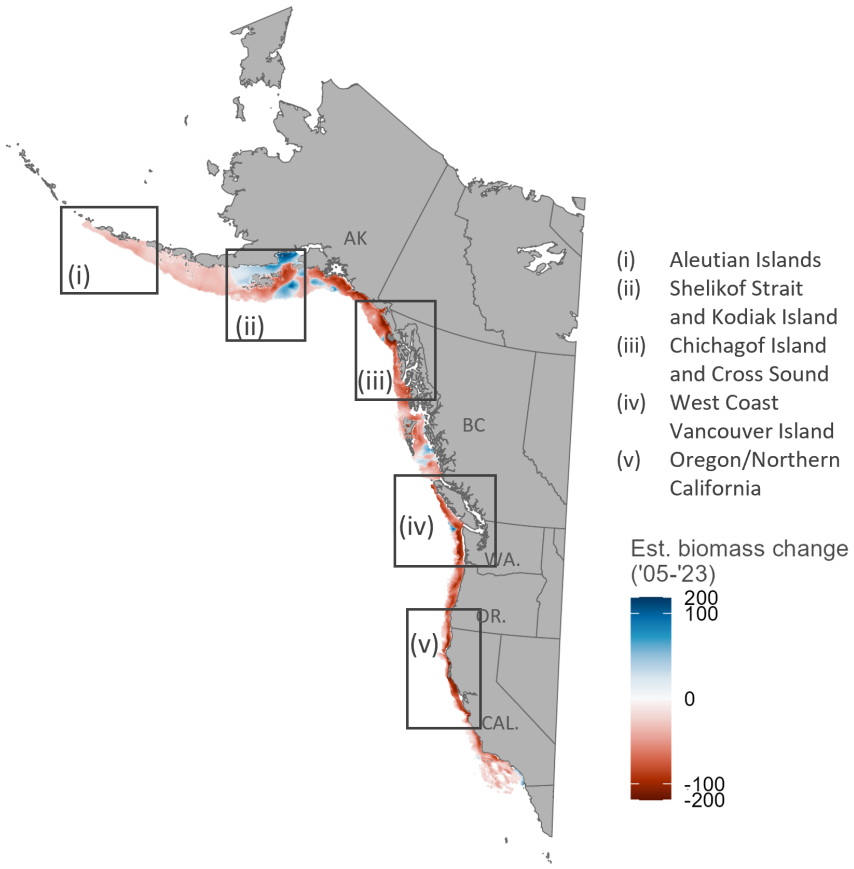

Figure S21: Areas highlighted in text. (i) Aleutian Islands, (ii) Sheilkof Strait and Kodiak Island, (iii) Chichagof Island and Cross Sound, (iv) West Coast Vancouver Island, and (v) Eureka, Oregon and Northern California. States and provinces are labeled according. Absolute change in combined biomass density from Figure 4 is plotted for reference.

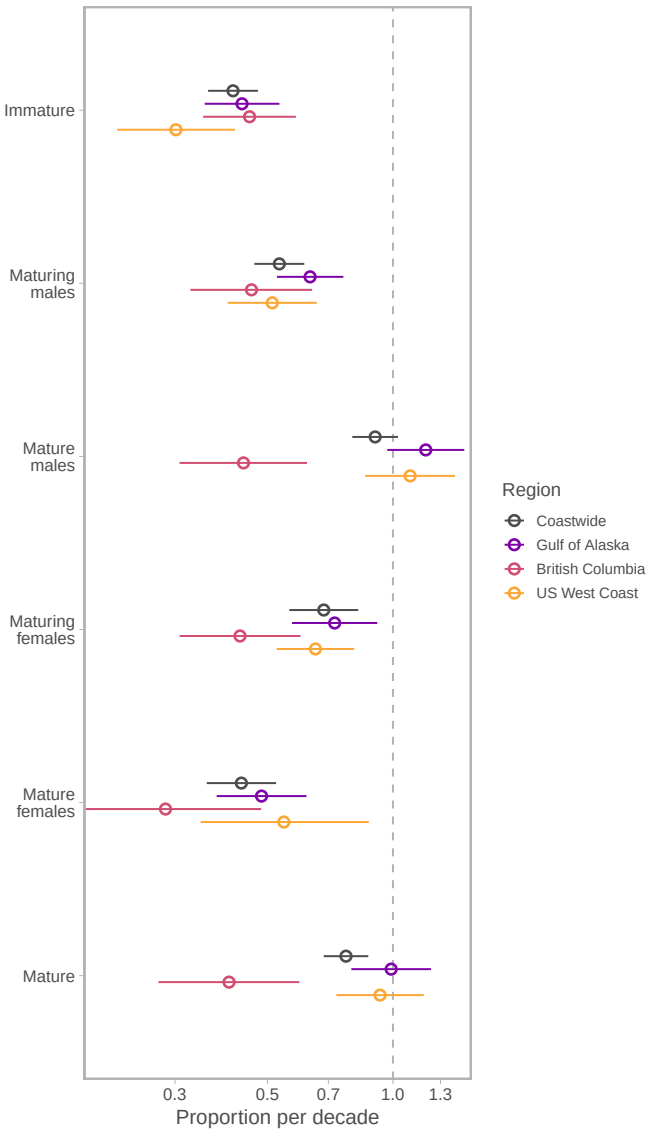

Figure S22: Coefficients for maturity groups by region. Immature, Maturing males, Mature male, Maturing females, and Mature females are the same as Figure 3(e) but includes mature individuals (mature females and mature males, combined) that was not included in main figure

.

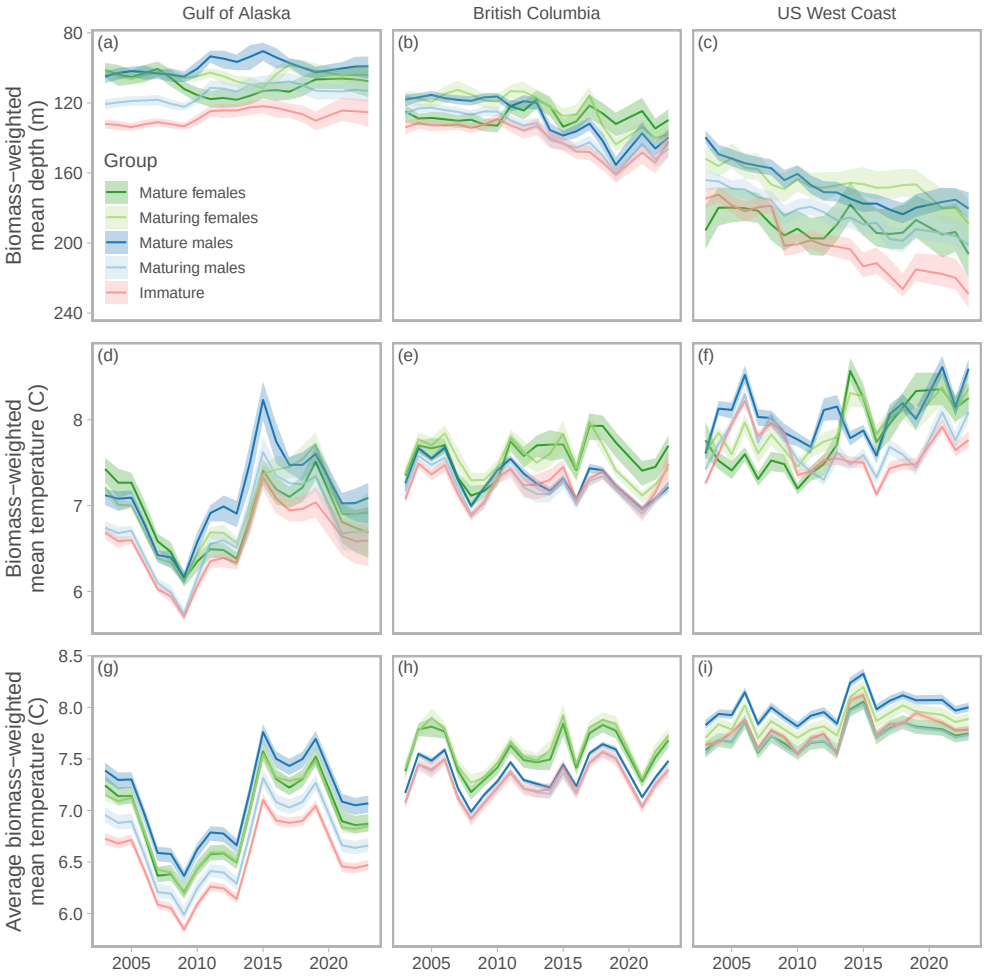

Figure S23: Biomass-weighted mean depth (a–c) and mean temperature (d–f) by region and maturity group. First two rows are the same as Figure 5 and lines represent the biomass-weighted mean depth or temperature and shaded ribbons represent 50% confidence intervals. This version adds the third row (g–i) where Dogfish distribution is kept constant at the average biomass per grid cell across time. The difference between rows d–f and rows g–i reflects the effect of changing Dogfish distribution.